Precise synthesis of rod-coil type miktoarm star copolymer containing poly(*n*-hexyl isocyanate) and aliphatic polyester

Toshifumi Satoh[1,*], Naoki Nishikawa[2], Daisuke Kawato[2], Daichi Suemasa[2], Sungmin Jung[3], Young Yong Kim[3], Moonhor Ree[3,*], and Toyoji Kakuchi[1,*]

[1]Fucluty of Engineering, Hokkaido University, N13W8, Kita-ku, Sapporo 060-8628, Japan

[2]Graduate School of Chemical Sciences and Engineering, Hokkaido University, N13W8, Kita-ku, Sapporo 060-8628, Japan

[3]Department of Chemistry, Division of Advanced Materials Science, Pohang Accelerator Laboratory, Center for Electro-Photo Behaviors in Advanced Molecular Systems, Polymer Research Institute, and BK School of Molecular Science, Pohang University of Science and Technology (POSTECH), Pohang 790-784, Republic of Korea

AUTHOR INFORMATION

Corresponding Authors

*E-mail satoh@poly-bm.eng.hokudai.ac.jp (T. Satoh), ree@postech.ac.kr (M. Ree), and kakuchi@poly-bm.eng.hokudai.ac.jp (T. Kakuchi).

Abstract

Well-defined hydroxyl end-functionalized poly(*n*-hexyl isocyanate), PHIC-$(OH)_2$ and PHIC-$(OH)_3$, as rod-type macroinitiators were synthesized by the Cu-catalyzed azide–alkyne cycloaddition reactions of azido end-functionalized PHIC with ethynyl alcohol derivatives. The PHIC-$(OH)_2$ and PHIC-$(OH)_3$ were suitable macroinitiators for the ring-opening polymerization of L-LA and ε-CL leading to the synthesis of novel rod-coil type miktoarm star copolymers, PHIC-*b*-$PLLA_2$, PHIC-*b*-$PLLA_3$, PHIC-*b*-PCL_2, and PHIC-*b*-PCL_3, with controlled molecular weights, narrow polydispersities, and controlled arm numbers. Additionally, the thermal and solution properties of the obtained miktoarm star copolymers along with the corresponding block copolymers, PHIC-*b*-PLLA and PHIC-*b*-PCL, were characterized by TGA, DSC, and DLS analyses.

Introduction

Miktoarm polymers are star-shaped copolymers composed of chemically different arm segments. Compared with corresponding linear block copolymers, miktoarm star copolymers exhibit dramatic differences in microphase separation in the solid as well as in solution.[1-9] Therefore, they have attracted much attention in recent years as novel functional materials with potential importance. Recently, a number of miktoarm star copolymers have been synthesized by various methods and studied on their properties.[10-45] As examples, Hadjichristidis and coworkers have used chlorosilane compounds to synthesize well-defined 3-, 4-, and 6-miktoarm star polymers through living anionic polymerization.[1-5,10-20] Hirao and coworker have developed a versatile synthetic strategy to create a wide variety of complex miktoarm stars, such as ABCDE-, ABCDEF-, ABCDEFG-, $ABCD_2$-, AB_2C_2-, $ABCD_2E_2$, $AB_2C_2D_2E_4$-, $AB_2C_2D_4E_4$-, $AB_2C_4D_8E_8$-, and $AB_2C_4D_8E_{16}$-type miktoarm stars.[7,9,28,29,35,36] Monteiro and coworker have synthesized 3-miktoarm star copolymers using a combination of the atom transfer radical polymerization and click reaction.[37] Unlike the above miktoarm star copolymers with

coil-like arms, the studies of miktoarm star copolymers containing rigid rod polymers are rare [46-55]; Lecommandoux and Taton et al. reported the synthesis and self-assembly in bulk of miktoarm star copolymers based on polystyrene and poly(glutamic acid) prepared by the combination of ATRP and ring-opening polymerization.[46] Lee et al. also reported the precise synthesis and the self-organization behavior of rod-coil type miktoarm star copolymers composed of poly(*n*-hexylisocyanate) (PHIC) and poly(ethylene glycol) and found that these polymers showed self-organization behaviors different from those of conventional coil-coil type miktoarm copolymers.[50] Although the miktoarm star copolymers containing a rod segment have the potential to exhibit unique properties, these synthetic methods still have limitations compared to those of the coil-coil type miktoarm star copolymers; therefore, expansion of the synthetic methods for the rod-coil type miktoarm star copolymers is needed. Recently, we reported that the clickable PHICs, azido and ethynyl end-functionalized PHICs, were suitable rod segments for the synthesis of well-defined macromolecular architectures based on a rod polymer, e.g., PHIC-*b*-poly(*N*-isopropyl acrylamide) (PNIPAM), PHIC-*b*-poly(L-lactide) (PLLA), and PHIC-*b*-poly(*ε*-caprolactone) (PCL) as rod-coil block copolymers and PHIC-star as a 4-arm rod star polymer.[56] The synthetic strategy with clickable PHICs is also useful for expanding the synthetic methods of well-defined rod-coil miktoarm star copolymers.

In the present study, we report the precise synthesis and self-assembly in solution of well-defined AB_2- and AB_3-type miktoarm star copolymers composed of PHIC as the A segment and PLLA or PCL as the B segment, as shown in Scheme 1. We designed these copolymers in order to compare the self-assembling property of the miktoarm star copolymers to that of diblock copolymers consisting of the same polymer segments. These AB_2- and AB_3-type miktoarm star copolymers were synthesized by the living ring-opening polymerization of L-lactide or *ε*-caprolactone with a hydroxyl end-functionalized PHIC (PHIC-$(OH)_2$ and PHIC-$(OH)_3$) as macroinitiators, respectively, which were obtained by the click reaction of the azido end-functionalized PHIC (PHIC−N_3) with ethynyl alcohol derivatives. We also studied the thermal and solution properties of these miktoarm star copolymers

along with the corresponding block copolymers, depending on their structure.

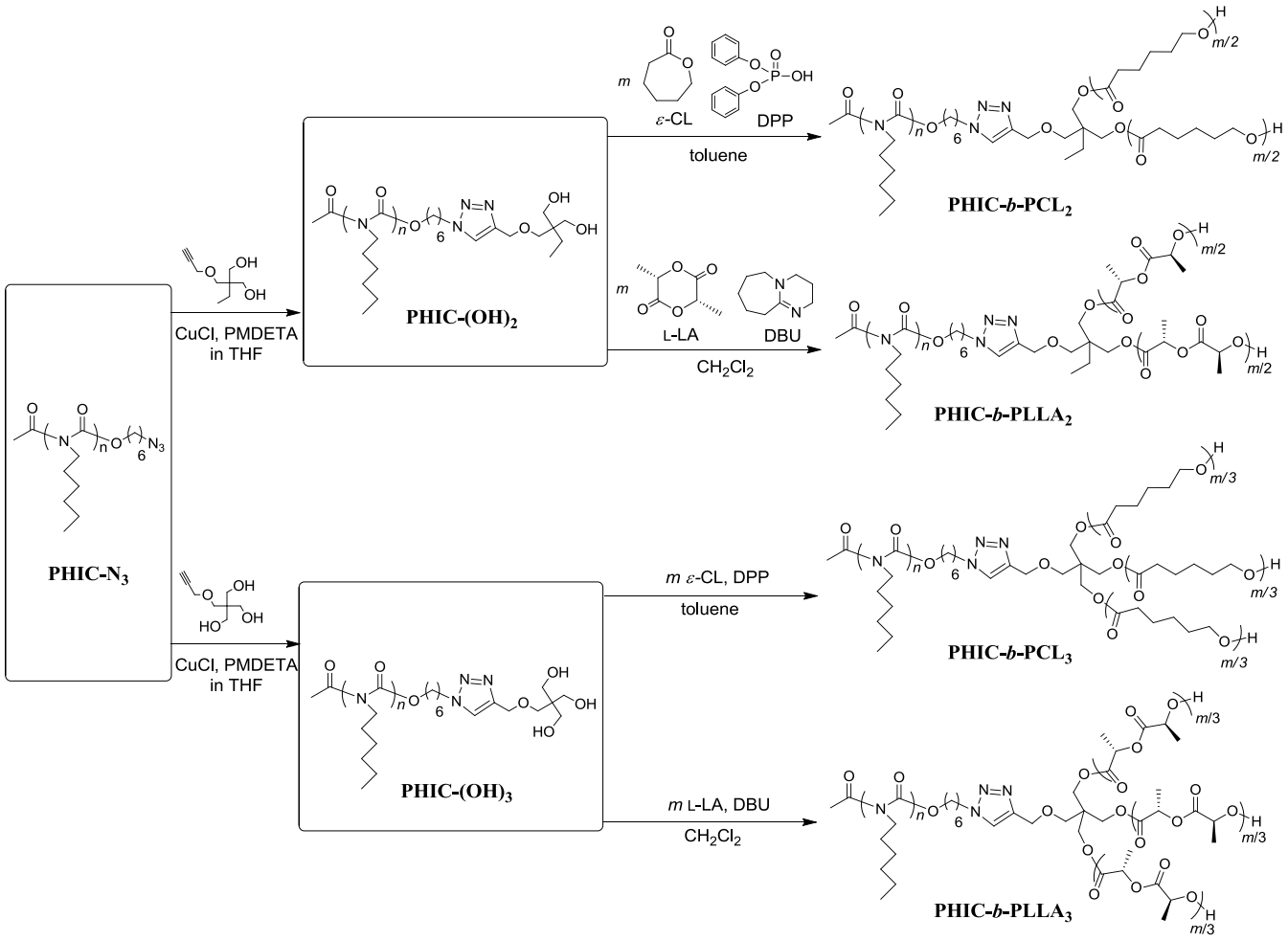

Scheme 1. Syntheses of hydroxyl end-functionalized PHICs (PHIC-$(OH)_2$ and PHIC-$(OH)_3$), PHIC-*b*-$PLLA_{2\sim3}$, and PHIC-*b*-$PCL_{2\sim3}$.

Experimental

Materials.

Dry toluene (>99.5%; Kanto Chemical Co., Inc., (Kanto)) was distilled over sodium benzophenone ketyl under an argon atmosphere. Dichloromethane (CH_2Cl_2; Kanto) was distilled over calcium hydride (CaH_2) under an argon atmosphere. *n*-Hexyl isocyanate (HIC; Tokyo Kasei Kogyo Co.,

Inc., (TCI)), ε-caprolactone (ε-CL; TCI), propargyl alcohol (TCI), 1,8-diazabicyclo[5.4.0]undec-7-ene (DBU; >98.0 %, Sigma Aldrich Chemical Co., (Aldrich)), and *N,N,N',N'',N''*-pentamethyldiethylene triamine (PMDETA; >98.0 %, TCI) were distilled over calcium hydride (CaH_2) under reduced pressure. L-Lactide (L-LA; TCI) was recrystallized twice from dry toluene. Trichloro(cyclopentadienyl)titanium (IV) ($CpTiCl_3$; Kanto), acetic anhydride (Kanto), boron trifluoride diethyl etherate ($BF_3{\cdot}OEt_2$; TCI), copper chloride(I) (CuCl; Aldrich, 99.995%), dry tetrahydrofuran (THF; Kanto), methanol (MeOH; Kanto), benzoic acid (Kanto), and diphenylphosphate (DPP; TCI) were used as received. 6-Azido-1-hexanol, 2-ethyl-2-[(prop-2-ynyloxy)methyl]propane-1,3-diol, and 2,2-bis-hydroxymethyl-3-prop-2-ynyloxy- propan-1-ol were synthesized using previously reported techniques. All other reagents were of synthetic grade and used without further purification.

Instruments.

The polymerization was carried out in an MBRAUN stainless steel glove box equipped with a gas purification system (molecular sieves and copper catalyst) in a dry argon atmosphere (H_2O, O_2 <1 ppm). The moisture and oxygen contents in the glove box were monitored by an MB-MO-SE 1 and an MB-OX-SE 1, respectively. The ^{1}H NMR spectra were recorded using a JEOL JNM-A400II instrument. The number-average molecular weight ($M_{n,NMR}$) was determined from the recorded ^{1}H NMR spectra. The size exclusion chromatography (SEC) was performed at 40 °C in THF (1.0 mL min^{-1}) using a Jasco GPC-900 system equipped with a set of two Shodex K-805 L columns (linear, 8 mm ×300 mm). The polydispersity (M_w/M_n) of the polymers was calculated on the basis of a polystyrene calibration. Matrix-assisted laser desorption/ionization time-of-flight mass spectrometry (MALDI-TOF MS) of the obtained polymers was performed using an Applied Biosystems Voyager-DE STR-H equipped with a 337-nm nitrogen laser (3-ns pulse width). Two hundred shots were accumulated for the spectra at a 20-kV acceleration voltage in the reflector mode and calibrated using polystyrene as the internal standard. Samples for the MALDI-TOF MS were prepared by mixing the polymer (5.0 g L^{-1}, 100 μL), a

matrix (Dithranol, 50 g L^{-1}, 50 μL), and a cationic agent (potassium trifluoroacetate, 25 g L^{-1}, 100 μL) in THF. The IR spectra were recorded using a Perkin Elmer Paragon 1000 FTIR spectrometer. Thermogravimetric analysis (TGA) and differential scanning calorimetry (DSC) measurements were carried out under a nitrogen atmosphere using a thermogravimeter (model TG/DTA 6200, Seiko Instruments, Japan) and a calorimeter (model DSC 6200, Seiko Instruments, Japan), respectively. A rate of 10.0 °C min^{-1} was employed for the heating and cooling runs. The dynamic light scattering (DLS) measurement was performed using an Otsuka Electronics FDLS-3000 light scattering spectrophotometer equipped with a solid state laser (λ = 532 nm, scattering angle = 90°). Before the measurement, the samples were filtered using 0.45-μm PTFE membrane filters to eliminate any dust particles. The data analysis was carried out using histogram methods including the CONTIN analysis.

Synthesis of PHIC-$(OH)_2$

To a 50-mL Schlenk flask, PHIC-N_3 (7.00 g, 1.40 mmol, $M_{n,NMR}$ = 5,000 g mol^{-1}, 1.0 eq.) and CuCl (415 mg, 4.20 mmol, 3.0 eq.) were added and dried under vacuum at room temperature overnight. Through a solution of PMDETA (1.76 mL, 8.40 mmol, 6.0 eq.), 2-ethyl-2-[(prop-2-ynyloxy)methyl]propane-1,3-diol (844 mg, 4.90 mmol, 3.5 eq.), and THF (6.70 ml) was bubbled flowing argon for 15 min and then introduced using a cannula. The reaction was allowed to proceed at room temperature for 48 h, then terminated by bubbling in air. The reaction mixture was purified by silica gel flash chromatography (THF) to remove the copper catalyst. The polymer was isolated by reprecipitation from the THF into cold methanol. Finally, the polymer was filtered and dried under vacuum to afford a light yellow powder; yield: 6.11 g, 87.3 %; $M_{n,NMR}$, 5,100, g mol^{-1}; $M_{n,SEC}$ (M_w/M_n) in THF, 6,100 g mol^{-1} (1.06). ^{1}H NMR ($CDCl_3$, 400MHz) δ (ppm): 7.48 (s, triazole ring), 4.81 (s, triazole ring-CH_2O), 4.36 (t, CH_2-triazole ring), 4.16 (br, C(=O)OCH_2), 3.86 (m, CCH_2OH), 3.66 (br, NCH_2), 2.28 (s, C(=O)CH_3), 1.59 (br, -$NCH_2CH_2(CH_2)_3CH_3$), 1.29 (br, $NCH_2CH_2(CH_2)_3CH_3$), and 0.88 (br, CH_2CH_3). The $M_{n,NMR}$ values were calculated from A(NCH_2)/A(C(=O)CH_3) × 3/2 × (M.W. of HIC)

+ 343, where $A(NCH_2)$ and $A(C(=O)CH_3)$ were the integral areas of signal at 3.66 ppm and that at 2.28 ppm, respectively. The value of 357 was the molecular weight of the residuals of terminal structures.

Synthesis of PHIC-$(OH)_3$

To a 50-mL Schlenk flask, PHIC-N_3 (7.00 g, 1.40 mmol, $M_{n,NMR}$ = 5,000 g mol^{-1}, 1.0 eq.) and CuCl (415 mg, 4.20 mmol, 3.0 eq.) were added and dried under vacuum at room temperature overnight. Through a solution of PMDETA (1.76 mL, 8.40 mmol, 6.0 eq.), 2,2-bis-hydroxymethyl-3-prop-2-ynyloxy-propan-1-ol (854 mg, 4.90 mmol, 3.5 eq.), and THF (6.70 ml) was bubbled flowing argon for 15 min and was then introduced using a cannula. The reaction was allowed to proceed at room temperature for 48 h, then terminated by bubbling in air. The reaction mixture was purified by silica gel flash chromatography (THF) to remove the copper catalyst. The polymer was isolated by reprecipitation from the THF into cold methanol. Finally, the polymer was filtered and dried under vacuum to afford a light yellow powder; yield: 5.83 g, 83.3 %; $M_{n,NMR}$, 5,200, g mol^{-1}; $M_{n,SEC}$ (M_w/M_n) in THF, 5,900 g mol^{-1} (1.06). ^{1}H NMR ($CDCl_3$, 400MHz) δ (ppm): 7.48 (s, triazole ring), 4.81 (s, triazole ring-CH_2O-), 4.36 (t, CH_2-triazole ring), 4.16 (br, C(=O)OCH_2), 3.86 (m, CCH_2OH), 3.66 (br, NCH_2), 2.28 (s, $C(=O)CH_3$), 1.59 (br, $NCH_2CH_2(CH_2)_3CH_3$), 1.29 (br, $NCH_2CH_2(CH_2)_3CH_3$), and 0.88 (br, CH_2CH_3). The $M_{n,NMR}$ values were calculated from $A(NCH_2)/A(C(=O)CH_3) \times 3/2 \times$ (M.W. of HIC) + 343, where $A(NCH_2)$ and $A(C(=O)CH_3)$ were the integral areas of signal at 3.66 ppm and that at 2.28 ppm, respectively. The value of 359 was the molecular weight of the residuals of terminal structures.

Synthesis of PHIC-*b*-$PLLA_2$

A typical procedure for the polymerization is as follows: In the glove box, PHIC-$(OH)_2$ (100 mg, 19.6 μmol, $M_{n,NMR}$ = 5,100, 1.0 eq.) was added to L-lactide (281 mg, 1.96 mmol, 100 eq.) and DBU (2.93 μL, 19.6 μmol, 1.0 eq.) in dry CH_2Cl_2 at 27 ºC. After 10 min, benzoic acid (3.60 mg, 29.4 μmol, 1.5 eq.) was added to quench the polymerization, and then the polymer was precipitated in 100 mL of

MeOH. The polymer was isolated by reprecipitation from the THF in cold MeOH/*n*-hexane (v/v = 9/1). Finally, the polymer was filtered and dried under vacuum to afford a white powder; yield: 281 mg, 74.1 %; $M_{n,NMR}$, 20,000 g mol^{-1}; $M_{n,SEC}$ (M_w/M_n) in THF, 23,300 g mol^{-1} (1.09). ^{1}H NMR ($CDCl_3$, 400MHz) δ (ppm): 7.48 (s, triazole ring), 5.19 (q, C(=O)C*H*CH$_3$O), 4.81 (s, triazole ring-C*H*$_2$O), 4.36 (t, C*H*$_2$-triazole ring), 4.16 (s, C(=O)OC*H*$_2$), 3.86 (s, CC*H*$_2$O), 3.66 (br, NC*H*$_2$), 2.28 (s, C(=O)C*H*$_3$), 1.62 (m, (C*H*$_2$)$_3$CH$_3$, OCH$_2$(C*H*$_2$)$_4$, C(=O)CHC*H*$_3$O), 1.29 (br, NCH$_2$C*H*$_2$), and 0.88 (br, CH$_2$C*H*$_3$). The $M_{n,NMR}$ values of PHIC-*b*-PLLA$_2$ were calculated from *A*(C(=O)C*H*CH$_3$O)/*A*(C(=O)C*H*$_3$) × 3/2 × (M.W. of L-LA) + $M_{n,NMR}$ of PHIC-(OH)$_2$, where *A*(C(=O)C*H*CH$_3$O) and *A*(C(=O)C*H*$_3$) were the integral areas of signal at 5.19 ppm and that at 2.28 ppm, respectively.

Synthesis of PHIC-*b*-PLLA$_3$

A typical procedure for the polymerization is as follows: In the glove box, PHIC-(OH)$_3$ (100 mg, 19.2 μmol, $M_{n,NMR}$ = 5,200, 1.0 eq.) was added to L-lactide (281 mg, 1.96 mmol, 100 eq.) and DBU (2.93 μl, 19.6 μmol, 1.0 eq.) in dry CH_2Cl_2 at 27 ºC. After 10 min, benzoic acid (3.60 mg, 29.4 μmol, 1.5 eq.) was added to quench the polymerization, and then the polymer was precipitated in 100 mL of MeOH. The polymer was isolated by reprecipitation from the THF in cold MeOH/*n*-hexane (v/v = 9/1). Finally, the polymer was filtered and dried under vacuum to afford a white powder; yield: 307 mg, 80.5 %; $M_{n,NMR}$, 20,200 g mol^{-1}; $M_{n,SEC}$ (M_w/M_n) in THF, 22,800 g mol^{-1} (1.08). ^{1}H NMR ($CDCl_3$, 400MHz) δ (ppm): 7.48 (s, triazole ring), 5.19 (q, C(=O)C*H*CH$_3$O), 4.81 (s, triazole ring-C*H*$_2$O-), 4.36 (t, C*H*$_2$-triazole ring), 4.16 (br, -C(=O)OC*H*$_2$-), 3.86 (br, -CC*H*$_2$O-), 3.66 (br, NC*H*$_2$), 2.28 (s, C(=O)C*H*$_3$), 1.62 (m, (C*H*$_2$)$_3$CH$_3$, OCH$_2$(C*H*$_2$)$_4$, C(=O)CHC*H*$_3$O), 1.29 (br, NCH$_2$C*H*$_2$), and 0.88 (br, CH$_2$C*H*$_3$). The $M_{n,NMR}$ values of PHIC-*b*-PLLA$_3$ were calculated from *A*(C(=O)C*H*CH$_3$O)/*A*(C(=O)C*H*$_3$) × 3/2 × (M.W. of L-LA) + $M_{n,NMR}$ of PHIC-(OH)$_3$, where *A*(C(=O)C*H*CH$_3$O) and *A*(C(=O)C*H*$_3$) were the integral areas of signal at 5.19 ppm and that at 2.28 ppm, respectively.

Synthesis of PHIC-*b*-PCL$_2$

A typical procedure for the polymerization is as follows: In the glove box, PHIC-(OH)$_2$ (300 mg, 58.8 μmol, $M_{n,NMR}$ = 5,100, 1.0 eq.) was added to ε-CL (0.978 ml, 8.82 mmol, 150 eq.) and the toluene stock solution of DPP (58.8 μL, 58.8 μmol, 1.00 mol·L^{-1} in toluene) in dry toluene at 27 ºC. After 24 h, Amberlyst A21 was added to quench the polymerization, and then the polymer was precipitated in 100 mL of MeOH. The polymer was isolated by reprecipitation from the THF in cold MeOH/*n*-hexane. Yield, 74.0%; $M_{n,NMR}$, 22,700 g mol^{-1}; $M_{n,SEC}$ (M_w/M_n) in THF, 34,300 g mol^{-1} (1.08). ^{1}H NMR ($CDCl_3$, 400MHz): δ (ppm) 7.50 (s, triazole ring), 4.59 (s,triazole ring-C*H*$_2$O), 4.36 (t, triazole ring-C*H*$_2$), 4.06 (t, C(=O)OC*H*$_2$-), 3.66 (br, NC*H*$_2$), 2.31 (t, C(=O)C*H*$_2$ and C(=O)C*H*$_3$)), 1.62 (m, NCH$_2$C*H*$_2$, C(=O)CH$_2$C*H*$_2$ and OCH$_2$C*H*$_2$), 1.29 (br, (C*H*$_2$)$_3$CH$_3$, C(=O)(CH$_2$)$_2$C*H*$_2$), and 0.88 (br, CH$_2$C*H*$_3$). The $M_{n,NMR}$ values of PHIC-*b*-PCL$_2$ were calculated from *A*(C(=O)OC*H*$_2$-)/*A*(triazole ring-C*H*$_2$O) × (M.W. of ε-CL) + $M_{n,NMR}$ of PHIC-(OH)$_2$, where *A*(C(=O)OC*H*$_2$-) and *A*(triazole ring-C*H*$_2$O) were the integral areas of signal at 4.06 ppm and that at 4.59 ppm, respectively.

Synthesis of PHIC-*b*-PCL$_3$

A typical procedure for the polymerization is as follows: In the glove box, PHIC-(OH)$_3$ (300 mg, 57.7 μmol, $M_{n,NMR}$ = 5,200, 1.0 eq.) was added to ε-CL (0.959 mL, 8.65 mmol, 150 eq.) and the toluene stock solution of DPP (57.7 μL, 57.7 μmol, 1.00 mol·L^{-1} in toluene) in dry toluene at 27 ºC. After 24 h, Amberlyst A21 was added to quench the polymerization, and the polymer was precipitated in 100 mL of MeOH. The polymer was isolated by reprecipitation from the THF in cold MeOH/*n*-hexane (v/v = 9/1). Yield, 85.1%; $M_{n,NMR}$, 23,500 g mol^{-1}; $M_{n,SEC}$ (M_w/M_n) in THF, 40,300 g mol^{-1} (1.05). ^{1}H NMR ($CDCl_3$, 400MHz): δ (ppm) 7.50 (s, triazole ring), 4.59 (s,triazole ring-C*H*$_2$O), 4.36 (t, triazole ring-C*H*$_2$), 4.06 (t, C(=O)OC*H*$_2$), 3.66 (br, NC*H*$_2$), 2.31 (t, C(=O)C*H*$_2$ and C(=O)C*H*$_3$)), 1.62 (m, NCH$_2$C*H*$_2$, C(=O)CH$_2$C*H*$_2$, OCH$_2$C*H*$_2$), 1.29 (br, (C*H*$_2$)$_3$CH$_3$, C(=O)(CH$_2$)$_2$C*H*$_2$), and 0.88 (br, CH$_2$C*H*$_3$). The $M_{n,NMR}$ values of PHIC-*b*-PCL$_3$ were calculated from *A*(C(=O)OC*H*$_2$-)/*A*(triazole

ring-CH_2O) × (M.W. of ε-CL) + $M_{n,NMR}$ of PHIC-$(OH)_3$, where A(C(=O)OCH_2-) and A(triazole ring-CH_2O) were the integral areas of signal at 4.06 ppm and that at 4.59 ppm, respectively.

Results and discussion

Synthesis of PHIC-$(OH)_2$ and PHIC-$(OH)_3$ via CuAAC reaction

In order to prepare the novel hydroxyl end-functionalized PHICs (PHIC-$(OH)_2$ and PHIC-$(OH)_3$), which can be used as macroinitiators for the ring-opening polymerization of the lactone and lactide leading to the novel well-defined rod-coil type miktoarm star copolymers, the copper-catalyzed azide–alkyne cycloaddition (CuAAC) reactions of the azido end-functionalized PHIC (PHIC-N_3) with ethynyl alcohol derivatives were carried out using CuCl and PMDETA in THF at room temperature (Scheme 1), according to our previous report for the preparation of PHIC-OH.[56] Table S1 (see Supplementary Information) summarizes the results of the CuAAC reactions along with those of PHIC-OH. The reactions were allowed to proceed for 48 h, and the polymers were obtained as light yellow powders in ca. 85 % isolated yield. Figures S1, S2, and 1-3 show the SEC traces, the IR spectra, the ^{1}H NMR spectra, and the MALDI-TOF MS spectra of the resultant polymers, respectively.

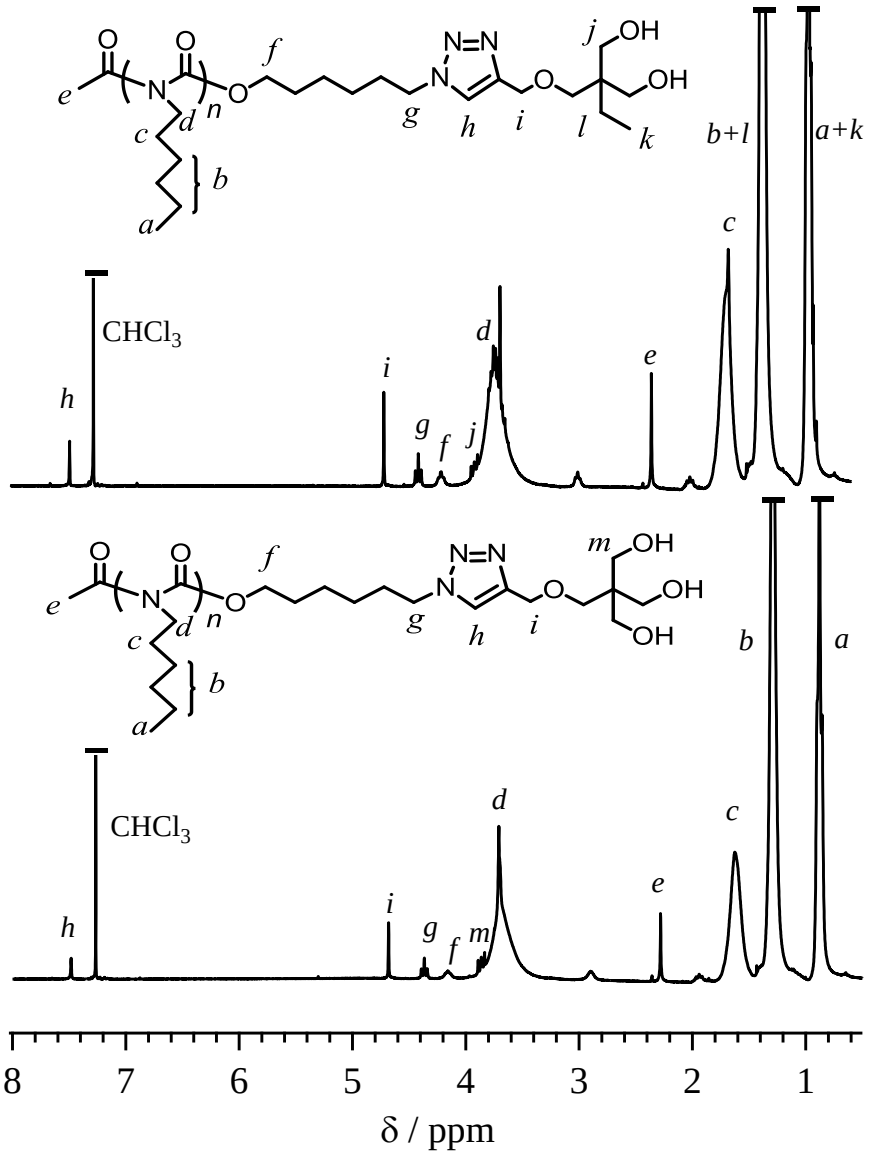

Figure 1. ^{1}H NMR spectra of PHIC-$(OH)_2$ (upper, $M_{n,NMR}$ = 5,100) and PHIC-$(OH)_3$ (lower, $M_{n,NMR}$ = 5,200) in $CDCl_3$.

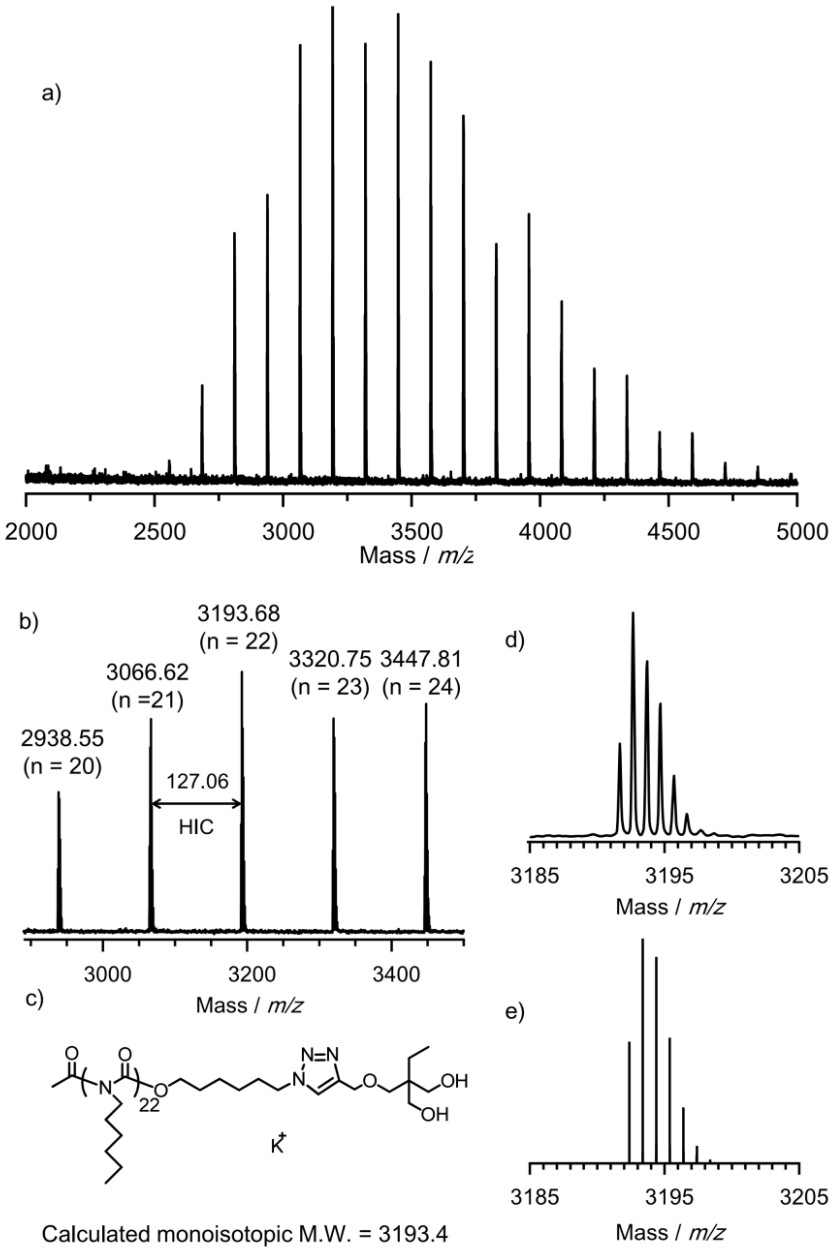

Figure 2. a) MALDI-TOF MS spectrum of PHIC-$(OH)_2$ ($M_{n,NMR}$ = 3,100), b) expansion of a), c) theoretical molecular weight and the predicted polymer structure of PHIC-$(OH)_2$, d) isotopic peak, and e) theoretical isotopic peak.

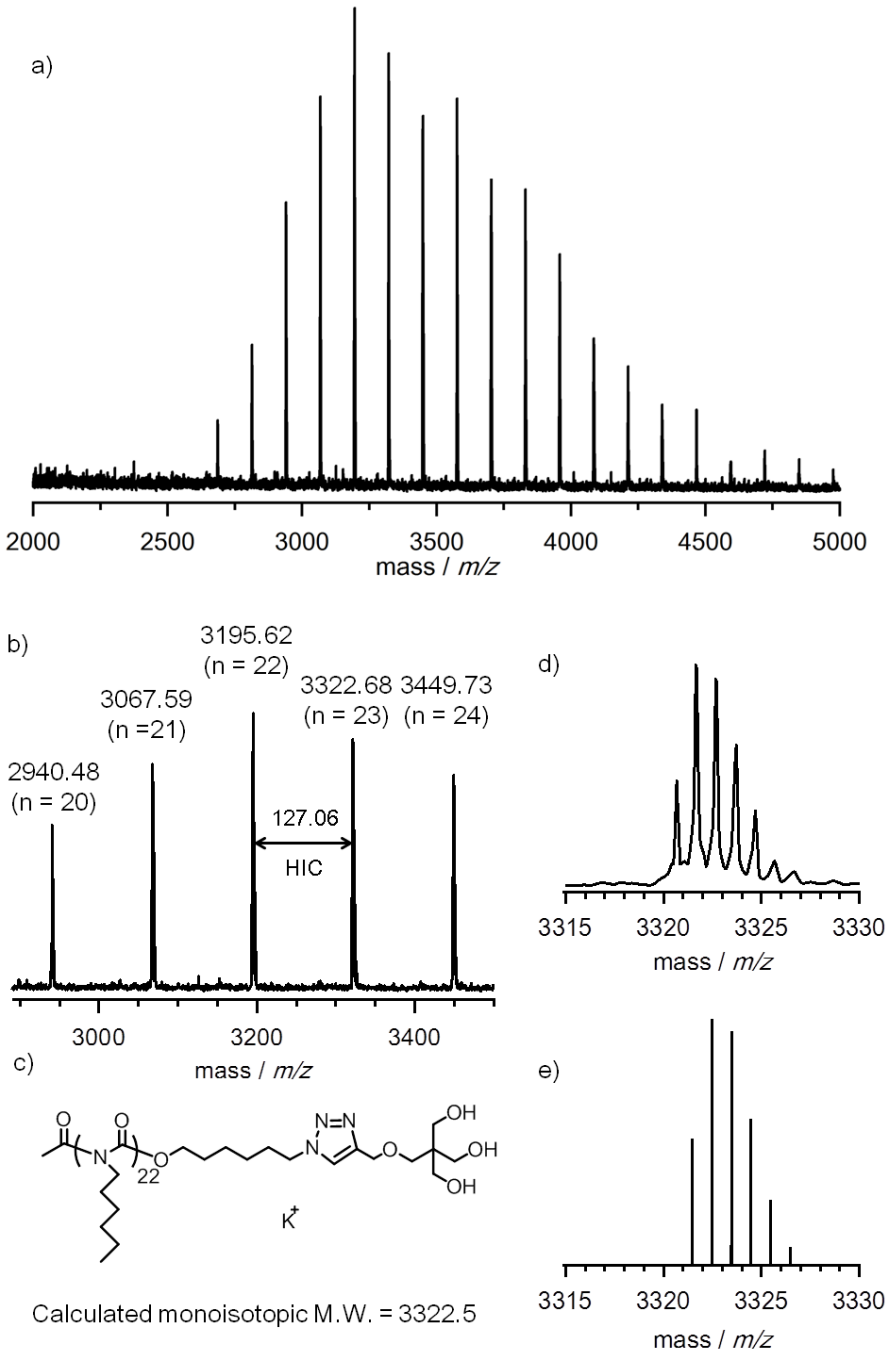

Figure 3. a) MALDI-TOF MS spectrum of PHIC-$(OH)_3$ ($M_{n,NMR}$ = 3,200), b) expansion of a), c) theoretical molecular weight and the predicted polymer structure of PHIC-$(OH)_3$, d) isotopic peak, and e) theoretical isotopic peak.

The SEC curve of the products displayed a monodispersed sharp peak with a narrow polydispersity (1.06 – 1.19) and there was no peak in the low molecular weight region (Figure S1 in Supplementary Information), strongly supporting the fact that the decomposition of PHIC did not proceed. In addition, the IR spectra of the products indicated the disappearance of the peak attributable to the azido group (2097 cm^{-1} in Figure S2), suggesting that there are no unreacted azido groups in the reaction products. Furthermore, in the ^1H NMR spectra of the products (Figure 1), the signals of the methylene protons (3.29 ppm) next to the azido group completely disappeared and the signal of the methine proton (*h* in Figure 1) in the triazole ring was observed at 7.52 ppm. Additionally, the signals due to the methylene protons (*i, g* and *j* (or *m*) in Figure 1) next to the triazole ring and hydroxyl group appeared at 4.81, 4.37, and 3.86 ppm, respectively. As further evidence, the MALDI-TOF MS spectra of PHIC-$(OH)_2$ and PHIC-$(OH)_3$ (Figures 2 and 3) showed only one series of peaks, which have a regular interval of ca. 127.06 for the molar mass corresponding to the repeating unit, and the peaks of the resultant polymers at m/z = 3193.68 for PHIC-$(OH)_2$ and 3322.68 for PHIC-$(OH)_3$ corresponded to the 22-mer of PHIC-$(OH)_2$ (3193.4, calcd. for $[M+K]^+$) and the 23-mer of PHIC-$(OH)_3$ (3322.5, calcd. for $[M+K]^+$), respectively. In addition, the isotopic distributions of these peaks were very similar to the theoretical ones. These results based on the SEC, ^1H NMR, IR, and MALDI-TOF MS analyses showed that the CuAAC reaction successfully proceeded and that the well-defined PHIC-$(OH)_2$ and PHIC-$(OH)_3$ were obtained as rod-like macroinitiators for the ring-opening polymerization.

Synthesis of PHIC-*b*-PLLA$_{2\sim3}$ and PHIC-*b*-PCL$_{2\sim3}$ using PHIC-(OH)$_{2\sim3}$ macroinitiators.

In order to synthesize the rod-coil type miktoarm star copolymer, the living ring-opening polymerization of the L-lactide (L-LA) and ε-caprolactone (ε-CL) with the PHIC-$(OH)_2$ or PHIC-$(OH)_3$ macroinitiator were carried out using the DBU[57] and DPP[58] catalysts, respectively (Scheme 1). There results are summarized in Tables 1 and 2, along with those of the corresponding block copolymers,

PHIC-*b*-PLLA and PHIC-*b*-PCL, using the PHIC-OH macroinitiator. The polymerizations homogeneously proceeded and the products were quantitatively obtained. The SEC traces of the products displayed unimodal peaks, which clearly shifted toward the higher molecular weight region as compared to the starting materials, as shown in Figures S3 and S4 (see Supplementary Information). In addition, the polydispersities of the obtained polymers were very narrow (1.04 – 1.14), as listed in Tables 1 and 2. In the ^{1}H NMR spectra of the obtained products, the signals due to PHIC and poly(L-lactide) (PLLA) or poly(ε-caprolactone) (PCL) were observed, as shown in Figures 4 and 5. The number-average molecular weights ($M_{n,NMR}$) of PHIC-*b*-PLLA$_2$ and PHIC-*b*-PLLA$_3$, estimated by NMR, well agreed with those of the calculated ($M_{n,clcd}$) based on the monomer conversion and initial ratio of [L-lactide]$_0$/[PHIC-(OH)$_{2\sim3}$]$_0$; $M_{n,NMR}$ = 20,000 g mol^{-1} and $M_{n,clcd}$ = 19,400 g mol^{-1} for PHIC-*b*-PLLA$_2$ and $M_{n,NMR}$ = 20,200 g mol^{-1} and $M_{n,clcd}$ = 19,500 g mol^{-1} for PHIC-*b*-PLLA$_3$. Similarly, the $M_{n,NMR}$'s of PHIC-*b*-PCL$_2$ and PHIC-*b*-PCL$_3$ were calculated to be 22,700 g mol^{-1} and 23,500 g mol^{-1} which well agreed with the $M_{n,clcd}$ of 22,200 g mol^{-1}and 22,300 g mol^{-1}, respectively. Furthermore, the composition of the block copolymers was easily controlled by changing the monomer and PHIC-(OH)$_{2\sim3}$ ratio ([M]$_0$/[PHIC-(OH)$_{2\sim3}$]$_0$). Based on the results, the ring-opening polymerizations of L-LA and ε-CL using the hydroxyl end-functionalized PHIC successfully proceeded to produce the well-defined rod-coil type miktoarm star copolymers, PHIC-*b*-PLLA$_{2\sim3}$ and PHIC-*b*-PCL$_{2\sim3}$, respectively, i.e., the hydroxyl end-functionalized PHICs for the ring-opening polymerization are very useful for synthesizing novel rod-coil type miktoarm star copolymers.

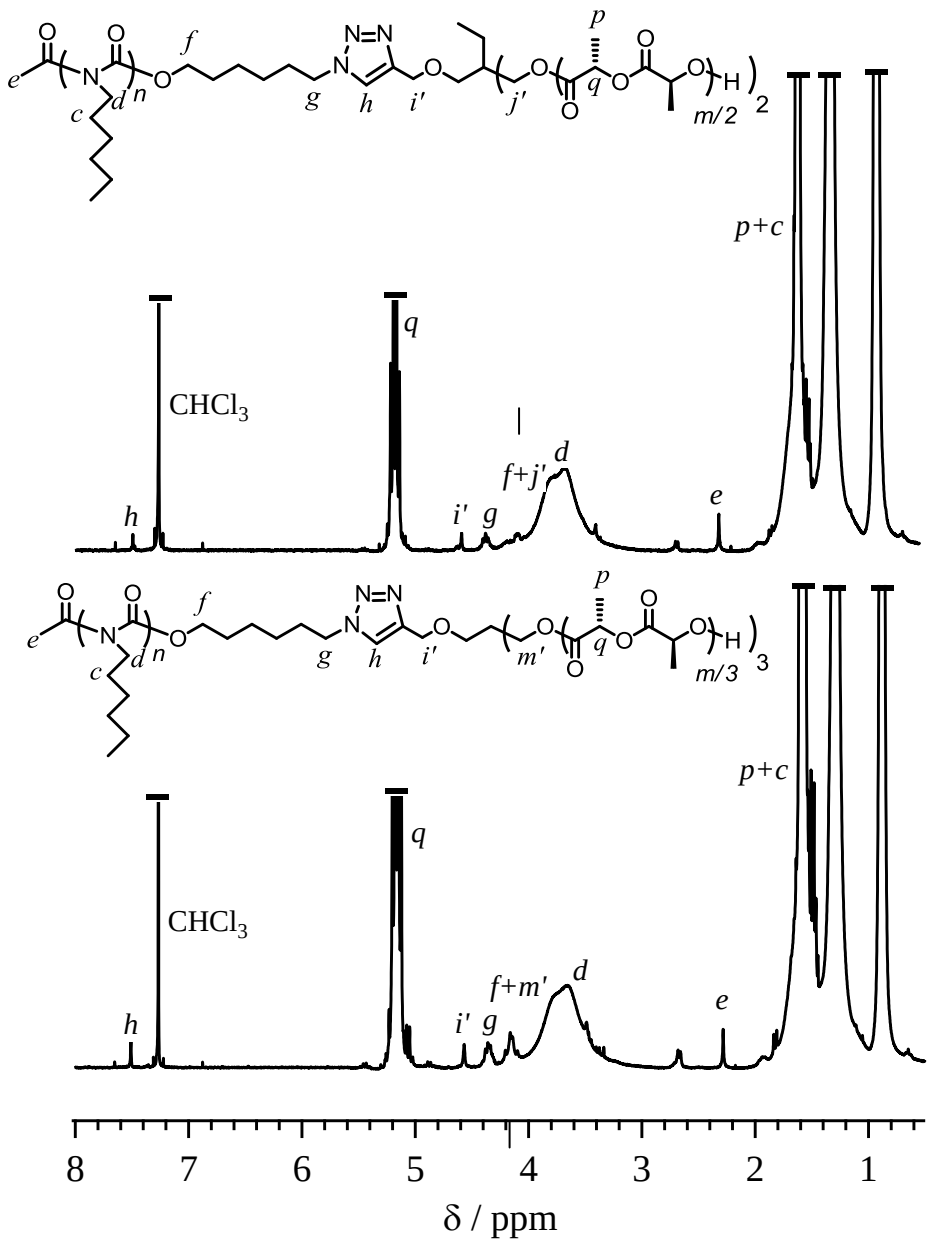

Figure 4. ^{1}H NMR spectra of PHIC-*b*-PLLA$_2$ (upper, $M_{n,NMR}$ = 20,000) and PHIC-*b*-PLLA$_3$ (lower, $M_{n,NMR}$ = 20,200) in $CDCl_3$.

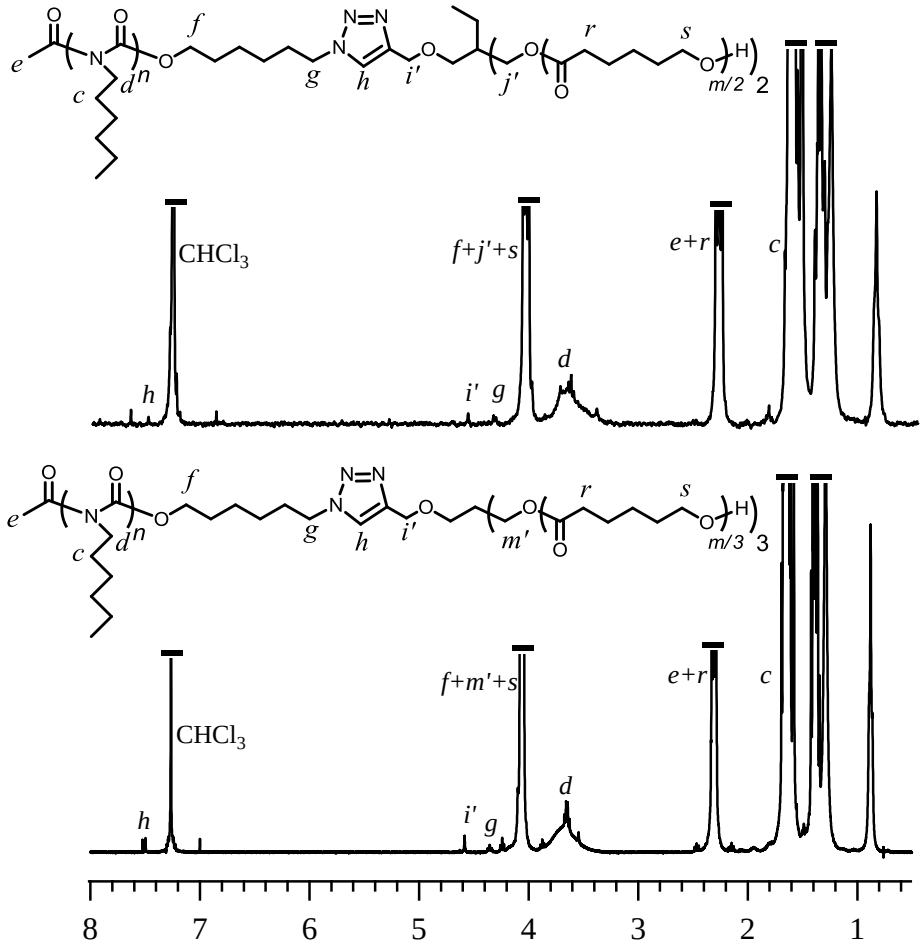

Figure 5. ^{1}H NMR spectrum of PHIC-*b*-PCL$_2$ (upper, $M_{n,NMR}$ = 22,700) and PHIC-*b*-PCL$_3$ (lower, $M_{n,NMR}$ = 23,500) in $CDCl_3$.

Thermal properties of PHIC-*b*-PLLA$_{1\sim3}$ and PHIC-*b*-PCL$_{1\sim3}$

The thermal properties of the PHIC-*b*-PLLA diblock copolymer, PHIC-*b*-PLLA$_2$ miktoarm star copolymer, and PHIC-*b*-PLLA$_3$ miktoarm star copolymer, which had an $M_{n,NMR}$ of ca. 20,000 g·mol^{-1} (PHIC: ca. 5,000 g·mol^{-1}; PLLA: ca. 15,000 g·mol^{-1}; f_{PHIC}: 0.30 - 0.31), were investigated under a nitrogen atmosphere by thermogravimetric analysis (TGA) and differential scanning calorimetry (DSC). The measured TGA thermograms are shown in Figures 6a-c. The PHIC-*b*-PLLA, PHIC-*b*-PLLA$_2$, and PHIC-*b*-PLLA$_3$ were found to undergo thermal degradation in a two-step manner. In the first-step, the degradation started at 187 °C (= $T_{d,1}$) for PHIC-*b*-PLLA, 191 °C for PHIC-*b*-PLLA$_2$, and 193 °C for PHIC-*b*-PLLA$_3$. In the second-step, the degradation began around 300 °C (= $T_{d,2}$) for all the three polymers. The TGA analysis found that the PHIC homopolymer revealed an onset degradation temperature T_d of around 190 °C while the PLLA hompolymer exhibited T_d = 300 °C (data not shown). Taking these facts into account, the first-step degradations were attributed to the degradation of the PHIC block in the polymers, whereas the second-step degradations were caused by the degradations of the PLLA blocks in the polymers.

Figures 6d-f show the DSC thermograms of the polymers. All the polymer samples revealed two endothermic peaks in the first heating run. The first peak appeared around 41 °C for PHIC-*b*-PLLA, 42 °C for PHIC-*b*-PLLA$_2$, and 42 °C for PHIC-*b*-PLLA$_3$. The second peak showed around 144 °C for PHIC-*b*-PLLA, 142 °C for PHIC-*b*-PLLA$_2$, and 140 °C for PHIC-*b*-PLLA$_3$. However, they all showed only one weak, broad exothermic peak over 50–130 °C in the subsequent cooling run from the melt. Furthermore, they also exhibited only one weak, broad endothermic peak in the range 35–55 °C in the second heating run. For the PHIC homopolymer, any phase transitions could not easily be discernible due to its rigid chain characteristics. In contrast, a thermally annealed sample of the PLLA homopolymer was found to reveal a glass transition around 43 °C (= T_g, glass transition temperature) and a melting transition around 145 °C (= T_m, melting point) (data not shown). With considering these results, the peaks observed in the DSC runs are attributed to phase transitions of the PLLA blocks in the

polymers. Therefore, one weak peak in the low temperature region and another strong peak in the high temperature region are originated from the glass transition and the melting transition of the PLLA blocks respectively. The glass transition of the PLLA block was also discernible in the cooling runs from the melt. However, in the cooling runs the PLLA blocks of the polymers could not reveal crystallization exothermic peak. PLLA is generally known to crystallize very slowly. Due to such the nature, in the cooling runs the PLLA blocks of the polymers could not have enough time to crystallize from the melts, resulting in no exothermic peak.

The thermal properties of the PHIC-*b*-$PCL_{1\sim3}$, which has a total molecular weight of ca. 22,000 $g{\cdot}mol^{-1}$ (PHIC: ca. 11,000 $g{\cdot}mol^{-1}$ and PCL: 11,000 $g{\cdot}mol^{-1}$; f_{PHIC}: 0.53 - 0.55), were also investigated. The polymers also showed thermal a two-step degradation behavior in the TGA runs (Figures 7a-c). With considering the degradation of the PHIC as well as of the PCL homopolymer (T_d = 320 °C), the first-step degradations ($T_{d,1}$ = 192 °C ~ 200 °C) were attributed to the PHIC block' degradation, whereas the second-step degradations were originated from the PCL blocks' degradation. Figures 7c-f show the DSC thermograms of the polymers. All the polymers revealed one strong peak in heating run as well as in cooling run from the melt. One endothermic peak of the PHIC-*b*-PCL, PHIC-*b*-PCL_2, and PHIC-*b*-PCL_3 was observed around 52 °C, 53 °C, and 48 °C, respectively. In addition, one exothermic peak of the PHIC-*b*-PCL, PHIC-*b*-PCL_2, and PHIC-*b*-PCL_3 is observed around 17 °C, 20 °C, and 11 °C, respectively. Taking into account consideration the PHIC homopolymer' rigid chain characteristics and the PCL hompopolymer' crystallization nature, the observed endothermic and exothermic peaks are originated from the melting and crystallization of the PCL block. In addition, the polymers showed a very weak, broad transition over the range −75 °C to −50 °C, which can be assigned as the glass transition of the PCL block. The glass transition was found to be very weak even for the polymer samples quenched from the melts; the T_g was estimated to be −71 °C for PHIC-*b*-PCL, −73 °C for PHIC-*b*-PCL_2, and −74 °C for PHIC-*b*-PCL_3 (Figure S5). The PCL blocks were found to undergo crystallization even during the quenching processes from the melts (Figure S6). Taking these results into

account, the weak glass transitions might be attributed to the PCL blocks' rapid crystallization nature.

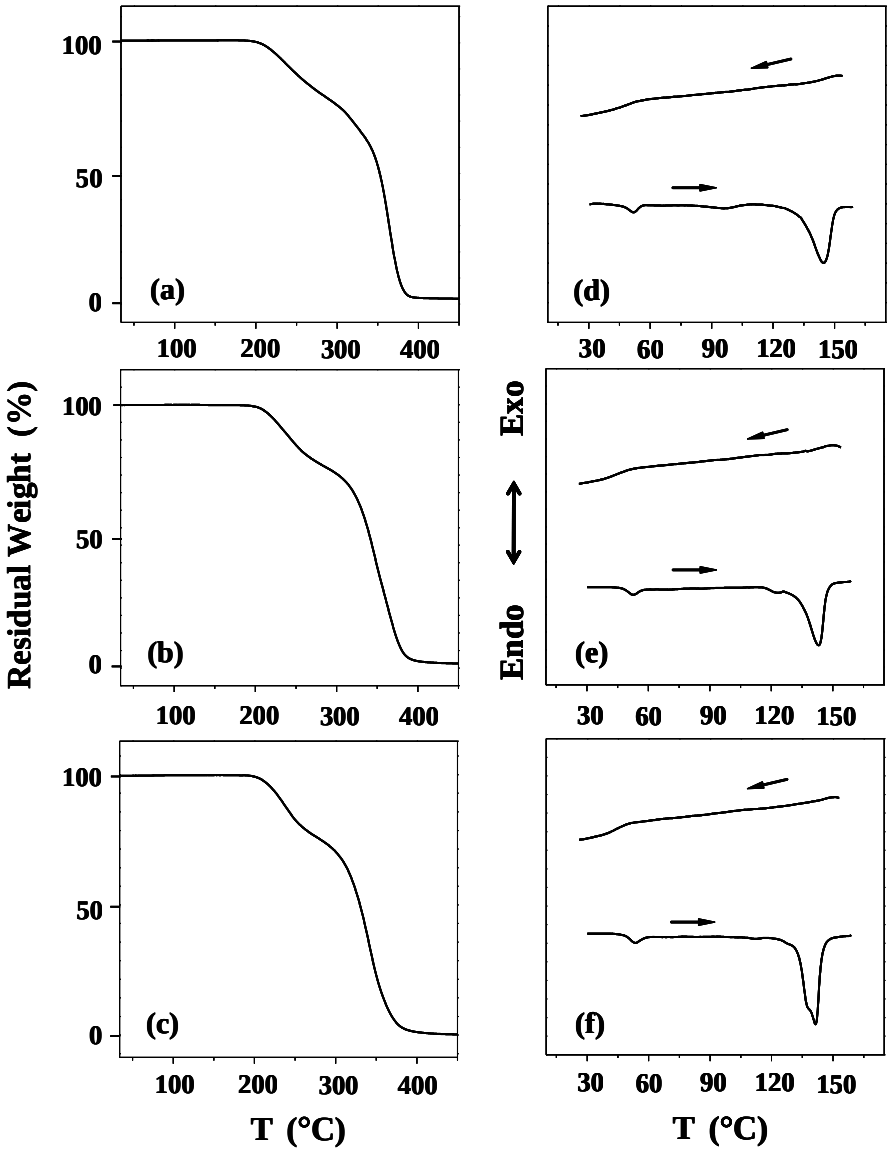

Figure 6. TGA and DSC results of PHIC-*b*-PLLA*1*. (a), (b) and (c) are TGA data of PHIC-*b*-PLLA ($M_{n,NMR}$ = 19,200, M_w/M_n = 1.07, f_{PHIC} = 0.31), PHIC-*b*-PLLA$_2$ ($M_{n,NMR}$ = 20,000, M_w/M_n = 1.09, f_{PHIC} = 0.30), and PHIC-*b*-PLLA$_3$ ($M_{n,NMR}$ = 20,200, M_w/M_n = 1.08, f_{PHIC} = 0.30), respectively. (d), (e), and (f) are DSC data of PHIC-*b*-PLLA, PHIC-*b*-PLLA$_2$, and PHIC-*b*-PLLA$_3$, respectively.

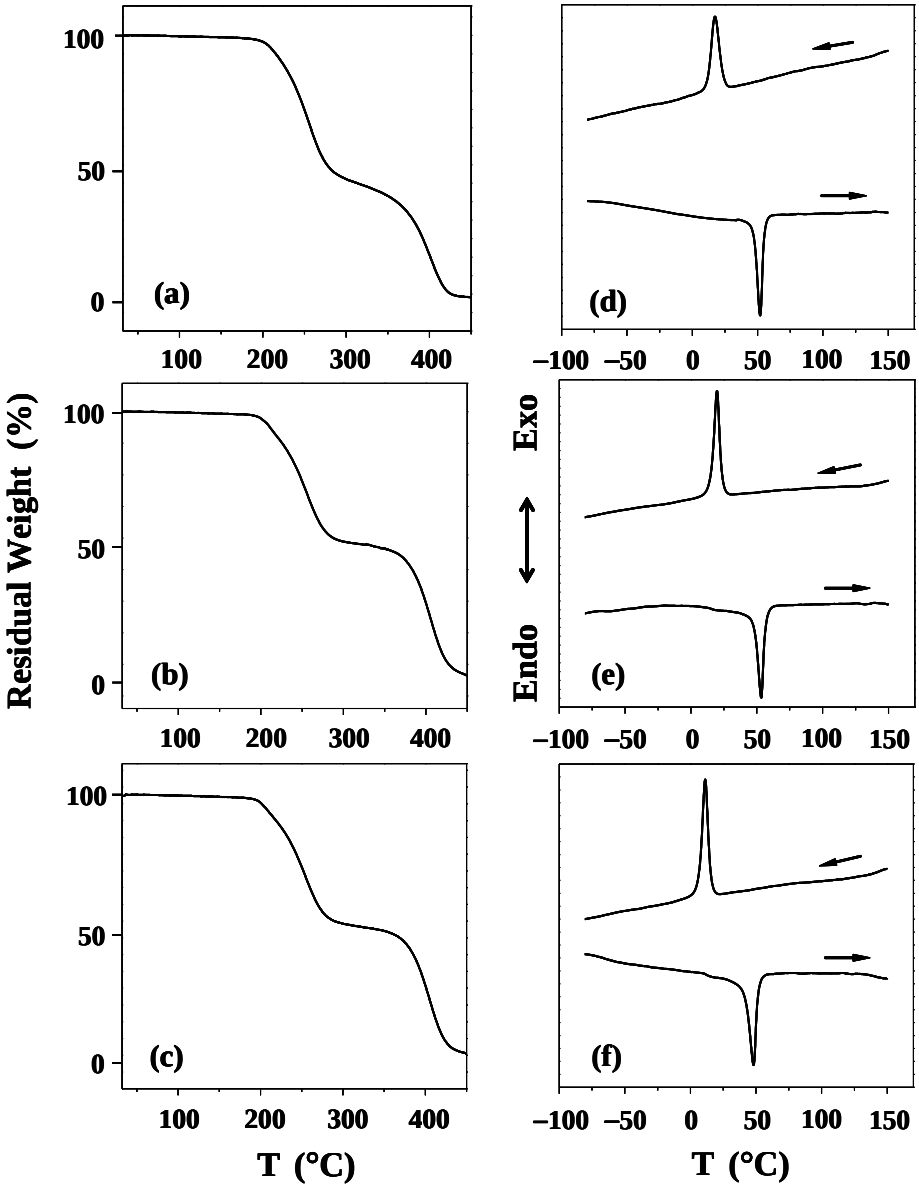

Figure 7. TGA and DSC results of PHIC-*b*-$PCL_{1\sim3}$. (a), (b) and (c) are TGA data of PHIC-*b*-PCL ($M_{n,NMR}$ = 22,200, M_w/M_n = 1.17, f_{PHIC} = 0.55), PHIC-*b*-PCL_2 ($M_{n,NMR}$ = 23,000, M_w/M_n = 1.12, f_{PHIC} = 0.53), and PHIC-*b*-PCL_3 ($M_{n,NMR}$ = 22,200, M_w/M_n = 1.14, f_{PHIC} = 0.54), respectively. (d), (e), and (f) are DSC data of PHIC-*b*-PCL, PHIC-*b*-PCL_2, and PHIC-*b*-PCL_3, respectively.

Solution properties of PHIC-*b*-$PLLA_{1\sim3}$ and PHIC-*b*-$PCL_{1\sim3}$

The solubility characteristics of PHIC-*b*-$PLLA_{1\sim3}$ and PHIC-*b*-$PCL_{1\sim3}$ were examined using various solvents and are summarized along with those of the PLLA, PCL, and PHIC homopolymers in

Table S2 (see Supplementary Information). PHIC-*b*-PLLA$_{1\sim3}$, PHIC-*b*-PCL$_{1\sim3}$, PLLA, and PCL were soluble in $CHCl_3$, THF, and DMF, but insoluble in hexane, while the PHIC homopolymer was soluble in $CHCl_3$, THF, and hexane, but insoluble in DMF. Based on these results, PHIC-*b*-PLLA$_{1\sim3}$ and PHIC-*b*-PCL$_{1\sim3}$ in DMF should form a micelle consisting of a PHIC core and PLLA (or PCL) shell. In fact, in the ^{1}H NMR spectra of PHIC-*b*-PLLA$_{1\sim3}$ and PHIC-*b*-PCL$_{1\sim3}$, the signals due to all protons appeared in $CDCl_3$, whereas the signals due to the PHIC segments did not appear in DMF (Figure 8). These results showed that the mobility of the PHIC protons was significantly limited because the PHIC segments in DMF were located on the inside of the micelle.

To confirm the solution structures of PHIC-*b*-PLLA$_{1\sim3}$ and PHIC-*b*-PCL$_{1\sim3}$, we performed dynamic light scattering (DLS) measurements at various concentrations in DMF (Figure 9). The weight-average hydrodynamic diameters (D_h) of PHIC-*b*-PLLA, PHIC-*b*-PLLA$_2$, and PHIC-*b*-PLLA$_3$ with the f_{PHIC} of 0.54-0.59, which had a molecular weight of ca. 20,000 g·mol^{-1}, were ca. 80 nm, 70 nm, and 45 nm, respectively, as shown in Figure 9b. The D_h values have no influence on the polymer concentration in the range from 0.02 to 2.0 g L^{-1} but drastically decreased below 0.02 g L^{-1}; the critical micelle concentrations (CMC) of these copolymers were below 0.01 g L^{-1} and increased with the increasing arm number of the PLLA chain. In contrast, the D_h values of PHIC-*b*-PLLA$_{1\text{-}3}$ with the f_{PHIC} of 0.30-0.31 (Figure 9a) were lower than those of the corresponding copolymers with the f_{PHIC} of 0.54-0.59, though these block copolymers have similar molecular weights (ca. 20,000 g mol^{-1}), indicating that the PHIC rod parts strongly affected the diameter of the micelle. Interestingly, The D_h values of PHIC-*b*-PLLA$_{1\sim3}$ decreased with the increasing arm number of the PLLA chain. This same tendency was observed for PHIC-*b*-PCL$_{1\sim3}$ in DMF, as shown in Figure 10. This phenomenon is considered to be influenced by the excluded volume effect of the PLLA (or PCL) chain, as shown in Figure 11, i.e., the bulkiness of the PLLA (or PCL) chains affected the micelle formation and PHIC-*b*-PLLA$_3$ (or PHIC-*b*-PCL$_3$) could not form micelle bigger than PHIC-*b*-PLLA and PHIC-*b*-PLLA$_2$ (or PHIC-*b*-PCL and PHIC-*b*-PCL$_2$). As a result, the micelle size can be controlled by

the arm number even for the same molecular weight and composition. This phenomenon should also affect the self-organization in the solid state, i.e., the domain size and structure can be controlled by the arm number.[59]

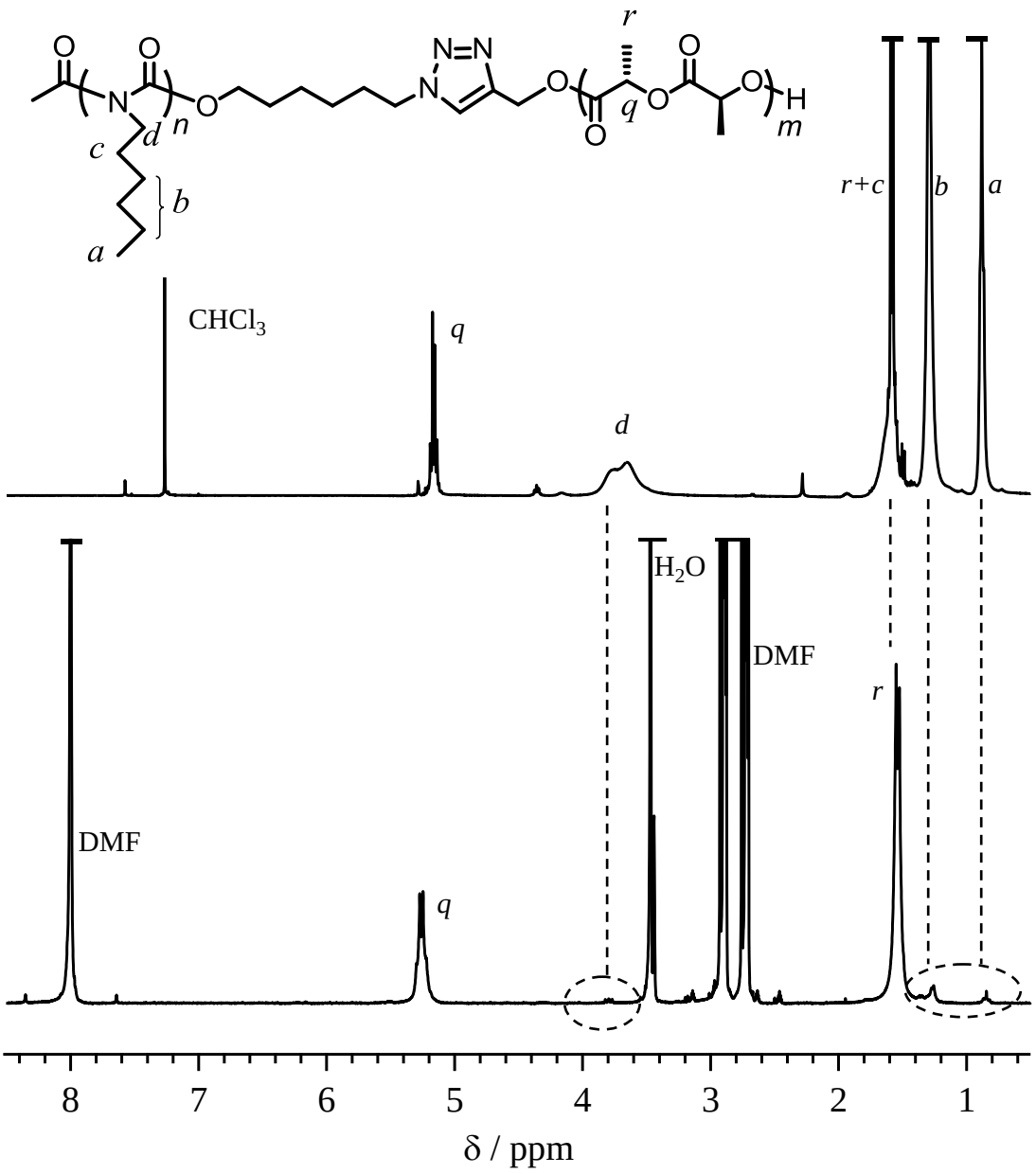

Figure 8. ^{1}H NMR spectra of PHIC-*b*-PLLA ($M_{n,NMR}$ = 19,200, M_w/M_n = 1.07, f_{PHIC} = 0.59, upper: in $CDCl_3$, lower: in DMF-d_7)

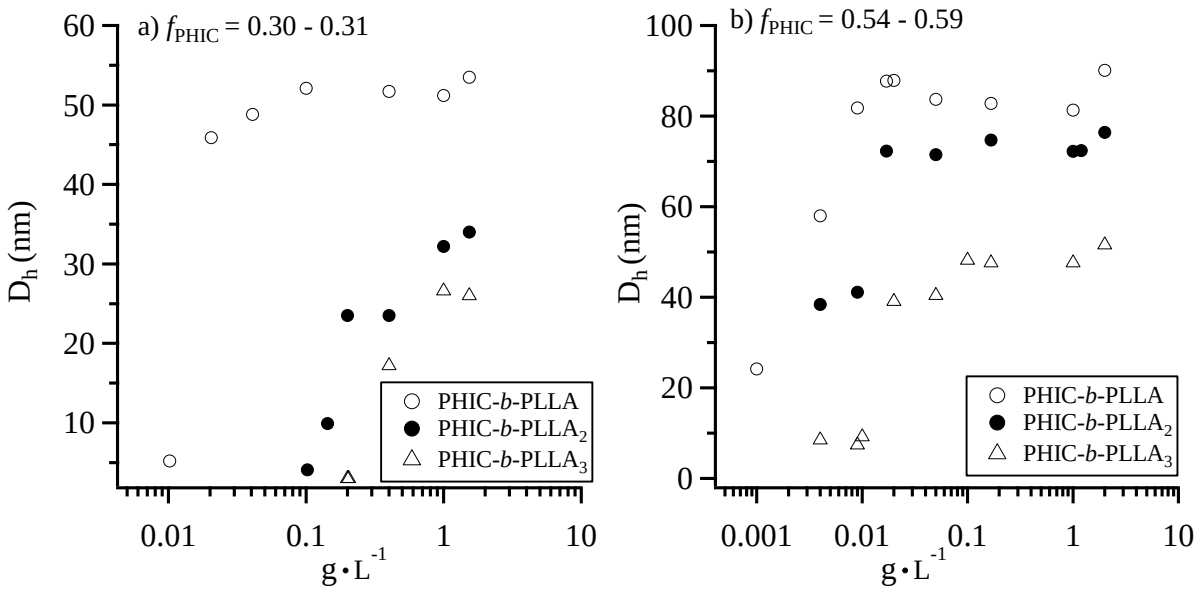

Figure 9. Hydrodynamic radius (D_h) measured by dynamic light scattering (DLS) of PHIC-*b*-PLLA$_{1\sim3}$ in DMF at 25 ˚C. a) f_{PHIC} = 0.30 - 0.31 (PHIC-*b*-PLLA: $M_{n,NMR}$ = 19,200, PHIC-*b*-PLLA$_2$: $M_{n,NMR}$ = 20,000, and PHIC-*b*-PLLA$_3$: $M_{n,NMR}$ = 20,200), b) f_{PHIC} = 0.54 - 0.59 (PHIC-*b*-PLLA: $M_{n,NMR}$ = 19,200, PHIC-*b*-PLLA$_2$: $M_{n,NMR}$ = 20,700, and PHIC-*b*-PLLA$_3$: $M_{n,NMR}$ = 19,700).

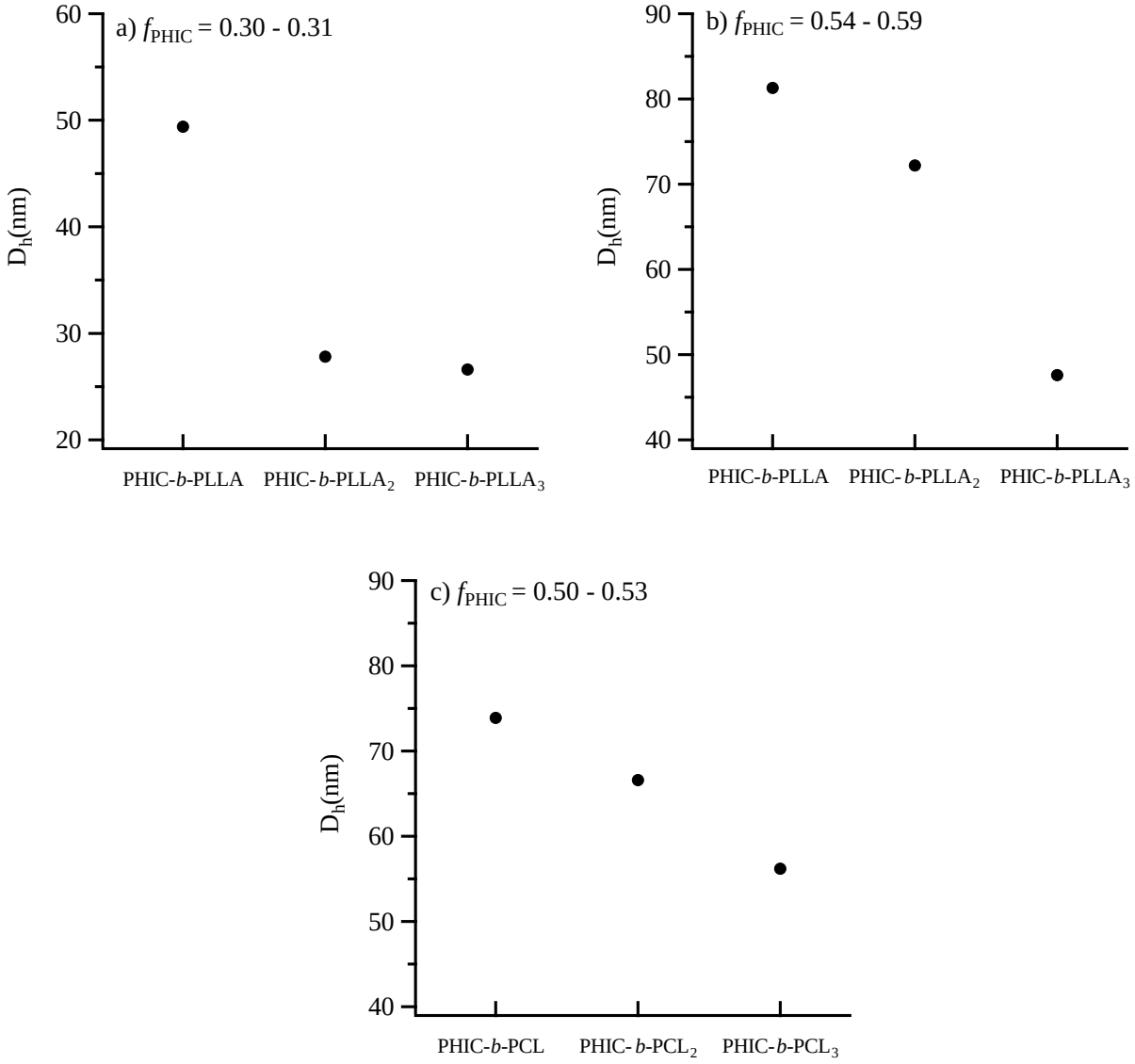

Figure 10. Hydrodynamic radius (D_h) measured by DLS of PHIC-*b*-PLLA$_{1\sim3}$ and PHIC-*b*-PCL$_{1\sim3}$ in DMF (1.0 g L^{-1} at 25 ˚C). a) f_{PHIC} = 0.30 - 0.31 (PHIC-*b*-PLLA: $M_{n,NMR}$ = 19,200, PHIC-*b*-PLLA$_2$: $M_{n,NMR}$ = 20,000, and PHIC-*b*-PLLA$_3$: $M_{n,NMR}$ = 20,200), b) f_{PHIC} = 0.54 - 0.59 (PHIC-*b*-PLLA: $M_{n,NMR}$ = 19,200, PHIC-*b*-PLLA$_2$: $M_{n,NMR}$ = 20,700, and PHIC-*b*-PLLA$_3$: $M_{n,NMR}$ = 19,700), and c) f_{PHIC} = 0.50

- 0.53 PHIC-*b*-PCL: $M_{n,NMR}$ = 20,900, PHIC-*b*-PCL_2: $M_{n,NMR}$ = 22,200, and PHIC-*b*-PCL_3: $M_{n,NMR}$ = 20,600).

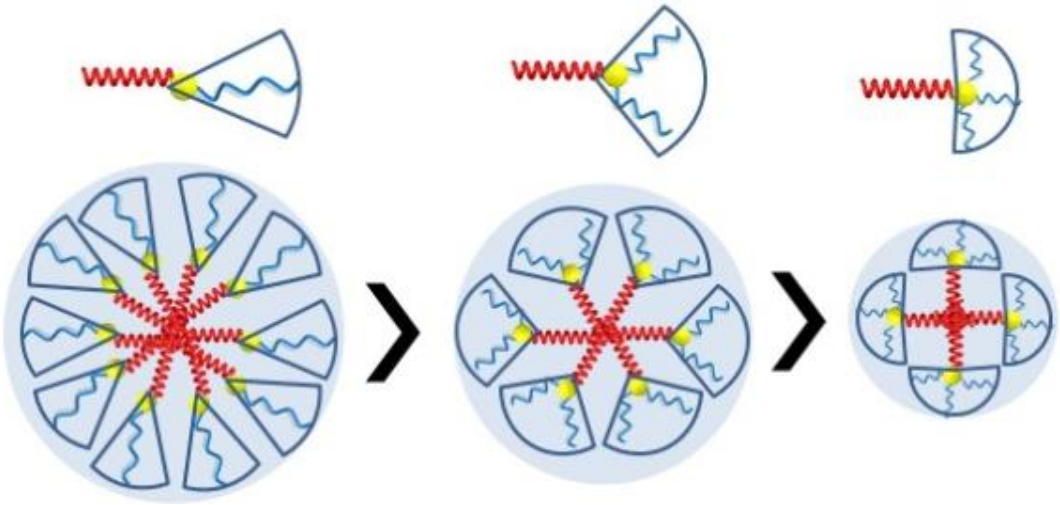

Figure 11. Proposed aggregation behavior of PHIC-*b*-$PLLA_{1\sim3}$ and PHIC-*b*-$PCL_{1\sim3}$ in DMF

Conclusions

The PHIC-$(OH)_{1\sim3}$, which were synthesized by the CuAAC reactions of PHIC-N_3 with ethynyl alcohol derivatives, were employed as rod-type macroinitiators for the ring-opening polymerization of L-LA and ε-CL leading to the synthesis of the PHIC-*b*-$PLLA_{1\sim3}$ and PHIC-*b*-$PCL_{1\sim3}$ block and miktoarm star copolymers. The well-defined products with controlled molecular weights, narrow polydispersities, and controlled arm numbers were obtained, i.e., the PHIC-$(OH)_{1\sim3}$ were suitable rod-type macroinitiators and generated a new possibility for the design and synthesis of a well-defined rod-coil type macromolecular architecture. The thermal properties of the PHIC-*b*-$PLLA_{1\sim3}$ and PHIC-*b*-$PCL_{1\sim3}$ block and miktoarm star copolymers were characterized by TGA and DSC analyses. The PHIC-*b*-PLLA, PHIC-*b*-$PLLA_2$, and PHIC-*b*-$PLLA_3$ revealed a two-step degradation process; the

PHIC block started degradation around around 190 °C while the PLLA block began degradation around 300 °C. The PHIC block could not show any discernible phase transitions due to the rigid chain nature. However, the PLLA block exhibited glass transition around 41 °C and melting transition around 142 °C. The PHIC-*b*-PCL, PHIC-*b*-PCL_2, and PHIC-*b*-PCL_3 also showed a two-step degradation process; the PHIC block started to degrade around 196 °C while the PCL block began to degrade around 320 °C. The PCL block revealed glass transition around be −72 °C and melting transition around 51 °C. The solution properties of PHIC-*b*-$PLLA_{1\sim3}$ and PHIC-*b*-$PCL_{1\sim3}$ were examined by DLS measurements in DMF. The D_h values of PHIC-*b*-$PLLA_{1\sim3}$ and PHIC-*b*-$PCL_{1\sim3}$ decreased with the increasing arm number of the PLLA and PCL chain due to the excluded volume effect of the PLLA and PCL chain. We are currently studying the self-organization behavior in the solid state of the PHIC-*b*-$PLLA_{1\sim3}$ and PHIC-*b*-$PCL_{1\sim3}$ using atomic force microscopy, electron microscopy and synchrotron grazing incidence X-ray scattering.

Acknowledgements

This work was financially supported by the MEXT (Japan) program "Strategic Molecular and Materials Chemistry through Innovative Coupling Reactions" of Hokkaido University and the MEXT Grant-in-Aid Project FY2011-2015 "Advanced Molecular Transformation by Organocatalysts". M. Ree acknowledges financial supports from the National Research Foundation (NRF) of Korea (Doyak Program 2011-0028678, Center for Electro-Photo Behaviors in Advanced Molecular Systems (2010-0001784) and Basic Research Grant No. 2010-0023396)) and the Ministry of Science, ICT & Future Planning (MSIP) (World Class University Programs (R31-2008-000-10059-0) and BK21 Program).

Notes and references

1 M. Pitsikalis, S. Pispas, J. W. Maysi, and N. Hadjichristidis. *Adv. Polym. Sci.,* 1998, **135**, 1.

2 N. Hadjichristidis, S. Pispas, M. Pitsikalis, C. Vlahos, and H. Iatrou, *Adv. Polym. Sci.* 1999, **142**, 71.

3 N. Hadjichristidis *J. Polym. Sci., Part A: Polym. Chem.,* 1999, **37**, 857.

4 N. Hadjichristidis, M. Pitsikalis, S. Pispas, and H. Iatrou. *Chem. Rev.*, 2001, **101**, 3747.

5 N. Hadjichristidis, M. Pitsikalis, and H. Iatrou, *Adv. Polym. Sci.*, 2005, **189**, 1.

6 K. Khanna, S, Varshney and A, Kakkar, *Polym. Chem.*, 2010, **1**, 1171

7 T. Higashihara, M. Hayashi, and Akira Hirao, *Prog. Polym. Sci.,* **36**, 2011, 323.

8 G. Ungar, C. Tschierske, V. Abetz, R. Holyst, M. A. Bates, F. Liu, M. Prehm, R. Kieffer, X. Zeng, M. Walker, B. Glettner, and A. Zywocinski, *Adv. Funct. Mater.* 2011, **21**, 1296.

9 S. Ito, R. Goseki, T. Ishizone, and A. Hirao, *European Polym. J.,* dx.doi.org/10.1016/j.eurpolymj.2013.05.014

10 H. Iatrou and N. Hadjichristidis, *Macromolecules*, 1992, **25**, 4649.

11 H. Iatrou and N. Hadjichristidis, *Macromolecules*, 1993, **26**, 2479.

12 J. Allgaier, R. N. Young, V. Efstratiadis and N. Hadjichristidis, *Macromolecules,* 1996, **29**, 1974–7.

13 A. Avgeropoulos, Y. Poulos, N. Hadjichristidis, and J. Roovers. *Macromolecules.* 1996, 29, 6076–8.

14 G. Velis and N. Hadjichristidis, *Macromolecules,* 1999, **32**, 534–6.

15 T. Tsoukatos and N. Hadjichristidis, *J. Polym. Chem. Part A: Polym. Chem.*, 2002, **40**, 2575–82.

16 A. Mavroudis, A. Avgeropoulos, N. Hadjichristidis, E. L. Thomas, and D. J. Lohse *Chem. Mater.*, 2003, **15**, 1976.

17 D. Cho, S. Park, T. Chang, A. Avgeropoulos and N. Hadjichristidis, *Eur. Polym. J.,* 2003, **39**, 2155.

18 P. G. Fragouli, H. Iatrou, N. Hadjichristidis, T. Sakurai and A. Hirao, *J. Polym. Sci., Part A: Polym. Chem.,* 2006, **44**, 614.

19 A. Mavroudis and N. Hadjichristidis, *Macromolecules,* 2006, **39**, 535.

20 A. Mavroudis, A. Avgeropoulos, N. Hadjichristidis, E. L. Thomas and D. J. Lohse, *Chem. Mater.*, 2006, **18**, 2164.

21 P. Fragouli, H. Iatrou, N. Hadichristidis, T. Sakurai, Y. Matsunaga and A. Hirao, *J. Polym. Sci., Part A: Polym. Chem.,* 2006, **44**, 6587.

22 P. G. Fragouli, H. Iatrou, N. Hadjichristidis, T. Sakurai, and A. Hirao, *J. Polym. Chem., Part A: Polym. Chem.,* 2006, **44**, 614–619.

23 M. Hayashi, K. Kojima, and A, Hirao, *Macromolecules*, 1999, **32**, 2425-2433.

24 A. Hirao and N. Haraguchi, *Macromolecules*, 2002, **35**, 7224.

25 A. Hirao and T. Higashihara, *Macromolecules*, 2002, **35**, 7238.

26 A. Hirao, M. Hayashi and A. Matsuo, *Polymer*, 2002, **43**, 7125.

27 A. Hirao and A. Matsuo, *Macromolecules*, 2003, **36**, 9742-9751.

28 T. Higashihara and A. Hirao, *J. Polym. Sci., Part A: Polym. Chem.*, 2004, **42**, 4535.

29 T. Higashihara, M. Nagura, K. Inoue, N. Haraguchi and A. Hirao, *Macromolecules*, 2005, **38**, 4577.

30 Y. L. Zhao, T. Higashihara, K. Sugiyama and A. Hirao, *J. Am. Chem. Soc.*, 2005, **127**, 14158.

31 A. Hirao, T. Higashihara, M. Nagura, and T. Sakurai, *Macromolecules*, 2006, **39**, 6081.

32 Y. L. Zhao, T. Higashihara, K. Sugiyama and A. Hirao, *Macromolecules*, 2007, **40**, 228.

33 A. Hirao, T. Higashihara and K. Inoue, *Macromolecules*, 2008, **41**, 3579.

34 T. Higashihara, T. Sakurai and A. Hirao, *Macromolecules*, 2009, **42**, 6006.

35 S. Ito, R. Goseki, S. Senda and A. Hirao, *Macromolecules*, 2012, **45**, 4997.

36 S. Ito, R. Goseki, T. Ishizone, S. Senda and A. Hirao, *Macromolecules*, 2013, **46**, 819.

37 M. R. Whittaker, C. N. Urbani and M. J. Monteiro, *J. Am. Chem. Soc.*, 2006, **128**, 11360.

38 R. Francis, B. Lepoittevin, D. Taton, and Y. Gnanou, *Macromolecules*, 2002, **35**, 9001.

39 Y. Cai, Y. Tang, and S. P. Armes, *Macromolecules*, 2004, **37**, 9728.

40 Y. Cai, C. Burguiere, S. P. Armes, *Chem. Commun.* 2004, 802.

41 Y. Miura, K, Yamaoka, M. A. Mannan, *Polymer*, 2006, **47**, 510.

42 K. Khanna, S. Varshney, and A. Kakkar, *Macromolecules*, 2010, **43**, 5688.

43 O. Altintas, A. P. Vogt, C. Barner-Kowollik and U. Tunca, *Polym. Chem.*, 2012, **3**, 34.

44 H. Durmaz, A. Sanyal, G. Hizal and U. Tunca, *Polym. Chem.*, 2012, **3**, 825.

45 U. S. Gunay, H. Durmaz, E. Gungor, A. Dag, G. Hizal and U. Tunca, *J. Polym. Chem., Part A: Polym. Chem.*, 2012, **50**, 729.

46 J. Babin, C. Leroy, S. Lecommandoux, R. Borsali, Y. Gnanou and D. Taton, *Chem. Commun.*, 2005, 1993.

47 J. Chen, X. Wang. X. Liao, H. Zhang, X. Wang, Q. Zhou, *Macromol. Rapid Commun*. 2006, **27**, 51.

48 A. Touris, K. Kostakis, S. Mourmouris, V. Kotzabasakis, M. Pitsikalis, and N. Hadjichristidis, *Macromolecules*, 2008, **41**, 2426.

49 J. Babin, D. Taton, M. Brinkmann, and S, Lecommandoux, *Macromolecules*, 2008, **41**, 1384.

50 M. S. Rahman, M. Changez, J.-W. Yoo, C. H. Lee, S. Samal, and J.-S. Lee, *Macromolecules*. 2008,

41, 7029.

51 Z. Ge and S Liu, *Macromol. Rapid Commun.*, 2009, **30**, 1523.

52 Y. Yamazaki, N. Ajioka, A. Yokoyama, and T. Yokozawa, *Macromolecules*, 2009, **42**, 606.

53 A. Gitsas, G. Floudas, M. Mondeshki, I. Lieberwirth, H. W. Spiess, H. Iatrou, N. Hadjichristidis, and A. Hirao, *Macromolecules*, 2010, **43**, 1874.

54 S. Junnila, N. Houbenov, S. Hanski, H. Iatrou, A. Hirao, N. Hadjichristidis, and O. Ikkala, *Macromolecules*, 2010, **43**, 9071.

55 J. G. Ray, A. J. Johnson, and D. A. Savin, *J. Polym. Sci., Part B: Polym. Phys.*, 2013, **51**, 508.

56 T. Satoh, R. Ihara, D. Kawato, N, Nishikawa, D. Suemasa, Y, Kondo, K. Fuchise, R. Sakai, and T. Kakuchi, *Macromolecules*, 2012, **45**, 3677.

57 B. G. G. Lohmeijer, R. C. Pratt, F. Leibfarth, J. W. Logan, D. A. Long, A. P. Dove, F. Nederberg, J. Choi, C. Wade, R. M. Waymouth, and J. L. Hedrick, *Macromolecules*, 2006, **39**, 8574.

58 K. Makiguchi, T. Satoh, and T. Kakuchi, *Macromolecules*, 2011, **44**, 1999.

59 T. Isono, I. Otsuka, Y. Kondo, S. Halila, S. Fort, C. Rochas, T. Satoh, R. Borsali, and T. Kakuchi, *Macromolecules*, 2013, **46**, 1461.

Supplementary Information

Tables S1 and S2, SEC and IR data of PHIC-$(OH)_{2\sim3}$ (Figures S1 and S2), SEC data of PHIC-*b*-$PLLA_{2\sim3}$ and PHIC-*b*-$PCL_{2\sim3}$ (Figures S3 and S4), and DSC data of PCL and PHIC-*b*-$PCL_{1\sim3}$ (Figures S5 and S6) are available free of charge via the Internet.

FIGURE CAPTIONS

Figure 1. ^{1}H NMR spectra of PHIC-$(OH)_2$ (upper, $M_{n,NMR}$ = 5,100) and PHIC-$(OH)_3$ (lower, $M_{n,NMR}$ =

5,200) in $CDCl_3$.

Figure 2. a) MALDI-TOF MS spectrum of PHIC-$(OH)_2$ ($M_{n,NMR}$ = 3,100), b) expansion of a), c) theoretical molecular weight and the predicted polymer structure of PHIC-$(OH)_2$, d) isotopic peak, and e) theoretical isotopic peak.

Figure 3. a) MALDI-TOF MS spectrum of PHIC-$(OH)_3$ ($M_{n,NMR}$ = 3,200), b) expantion of a), c) theoretical molecular weight and the predicted polymer structure of PHIC-$(OH)_3$, d) isotopic peak, and e) theoretical isotopic peak.

Figure 4. ^{1}H NMR spectra of PHIC-*b*-$PLLA_2$ (upper, $M_{n,NMR}$ = 20,000) and PHIC-*b*-$PLLA_3$ (lower, $M_{n,NMR}$ = 20,200) in $CDCl_3$.

Figure 5. ^{1}H NMR spectrum of PHIC-*b*-PCL_2 (upper, $M_{n,NMR}$ = 22,700) and PHIC-*b*-PCL_3 (lower, $M_{n,NMR}$ = 23,500) in $CDCl_3$.

Figure 6. TGA and DSC results of PHIC-*b*-$PLLA_{1\sim3}$. (a), (b) and (c) are TGA data of PHIC-*b*-PLLA ($M_{n,NMR}$ = 19,200, M_w/M_n = 1.07, f_{PHIC} = 0.28), PHIC-*b*-$PLLA_2$ ($M_{n,NMR}$ = 20,000, M_w/M_n = 1.09, f_{PHIC} = 0.27), and PHIC-*b*-$PLLA_3$ ($M_{n,NMR}$ = 20,200, M_w/M_n = 1.08, f_{PHIC} = 0.27), respectively. (d), (e), and (f) are DSC data of PHIC-*b*-PLLA, PHIC-*b*-$PLLA_2$, and PHIC-*b*-$PLLA_3$, respectively.

Figure 7. TGA and DSC results of PHIC-*b*-$PCL_{1\sim3}$. (a), (b) and (c) are TGA data of PHIC-*b*-PCL

($M_{n,NMR}$ = 22,200, M_w/M_n = 1.17, f_{PHIC} = 0.55), PHIC-*b*-PCL_2 ($M_{n,NMR}$ = 23,000, M_w/M_n = 1.12, f_{PHIC} = 0.53), and PHIC-*b*-PCL_3 ($M_{n,NMR}$ = 22,200, M_w/M_n = 1.14, f_{PHIC} = 0.54), respectively. (d), (e), and (f) are DSC data of PHIC-*b*-PCL, PHIC-*b*-PCL_2, and PHIC-*b*-PCL_3, respectively.

Figure 8. ^{1}H NMR spectra of PHIC-*b*-PLLA ($M_{n,NMR}$ = 19,200, M_w/M_n = 1.07, f_{PHIC} = 0.59, upper: in $CDCl_3$, lower: in DMF-d_7)

Figure 9. Hydrodynamic radius (D_h) measured by dynamic light scattering (DLS) of PHIC-*b*-$PLLA_{1\sim3}$ in DMF at 25 ˚C. a) f_{PHIC} = 0.30 - 0.31 (PHIC-*b*-PLLA: $M_{n,NMR}$ = 19,200, PHIC-*b*-$PLLA_2$: $M_{n,NMR}$ = 20,000, and PHIC-*b*-$PLLA_3$: $M_{n,NMR}$ = 20,200), b) f_{PHIC} = 0.54 - 0.59 (PHIC-*b*-PLLA: $M_{n,NMR}$ = 19,200, PHIC-*b*-$PLLA_2$: $M_{n,NMR}$ = 20,700, and PHIC-*b*-$PLLA_3$: $M_{n,NMR}$ = 19,700).

Figure 10. Hydrodynamic radius (D_h) measured by DLS of PHIC-*b*-$PLLA_{1\sim3}$ and PHIC-*b*-$PCL_{1\sim3}$ in DMF (1.0 g L^{-1} at 25 ˚C). a) f_{PHIC} = 0.30 - 0.31 (PHIC-*b*-PLLA: $M_{n,NMR}$ = 19,200, PHIC-*b*-$PLLA_2$: $M_{n,NMR}$ = 20,000, and PHIC-*b*-$PLLA_3$: $M_{n,NMR}$ = 20,200), b) f_{PHIC} = 0.54 - 0.59 (PHIC-*b*-PLLA: $M_{n,NMR}$ = 19,200, PHIC-*b*-$PLLA_2$: $M_{n,NMR}$ = 20,700, and PHIC-*b*-$PLLA_3$: $M_{n,NMR}$ = 19,700), and c) f_{PHIC} = 0.50 - 0.53 PHIC-*b*-PCL: $M_{n,NMR}$ = 20,900, PHIC-*b*-PCL_2: $M_{n,NMR}$ = 22,200, and PHIC-*b*-PCL_3: $M_{n,NMR}$ = 20,600).

Figure 11. Proposed aggregation behavior of PHIC-*b*-$PLLA_{1\sim3}$ and PHIC-*b*-$PCL_{1\sim3}$ in DMF

Table 1. Synthesis of PHIC-*b*-PLLA$_{1\sim3}$ using PHIC macroinitiators [a]

PHIC macroinitiator		$[M]_0/[I]_0$	block copolymer				
Structure	$M_{n,NMR}$ [b] (M_w/M_n [c])		Structure	$M_{n,clcd.}$ [d]	$M_{n,NMR}$ [b]	M_w/M_n [c]	f_{PHIC} [e]
PHIC-OH	5,100 (1.06)	100	PHIC-*b*-PLLA	19,400	19,200	1.07	0.31
	10,300 (1.13)	35		15,300	14,800	1.08	0.74
	10,300 (1.13)	70		20,400	19,200	1.07	0.59
PHIC-$(OH)_2$	5,100 (1.06)	100	PHIC-*b*-$PLLA_2$	19,400	20,000	1.09	0.30
	10,900 (1.13)	35		16,000	15,500	1.11	0.75
	10,900 (1.13)	70		21,000	20,700	1.12	0.59
PHIC-$(OH)_3$	5,200 (1.06)	100	PHIC-*b*-$PLLA_3$	19,500	20,200	1.08	0.30
	9,600 (1.16)	35		14,600	14,100	1.09	0.73
	9,600 (1.16)	70		19,700	19,700	1.08	0.54

[a] Polymerization conditions: monomer (M), L-lactide; solvent, dry-CH_2Cl_2; initiator (I), PHIC macroinitiator; $[M]_0$ = 1.0 mol·L^{-1}; catalyst, DBU; $[DBU]_0/[M]_0$ = 0.01; time 10 min; temp., 27 ˚C.; atmosphere, Ar.; conv., >99. [b] Determined by ^{1}H NMR spectrum in $CDCl_3$. [c] Determined by SEC in THF using PSt standards. [d] $M_{n,clcd} = ([M]_0/[I]_0) \times$ conv. × (M.W. of monomer) + $M_{n,\ initiator.}$ [e] $f_{PHIC} = (M_{n,NMR,PHIC} / d_{PHIC})/(M_{n,NMR,PHIC}/ d_{PHIC} + M_{n,NMR,PLLA}/ d_{PLLA})$, d_{PHIC} =1.00 and d_{PLLA}=1.25.

Table 2. Synthesis of PHIC-*b*-$PCL_{1\sim3}$ using PHIC macroinitiators.[a]

PHIC macroinitiator		$[M]_0/[I]_0$	time (h)	block copolymer				
Structure	$M_{n,NMR}$ [b] (M_w/M_n [c])			Structure	$M_{n,clcd.}$ [d]	$M_{n,NMR}$ [b]	M_w/M_n [c]	f_{PHIC} [e]
PHIC-OH	5,100 (1.06)	150	24	PHIC-*b*-PCL	22,200	21700	1.04	0.25
	10,300 (1.13)	90	16		20,600	20,900	1.07	0.53
	11,400 (1.19)	45	8		17000	16700	1.19	0.71
	11,400 (1.19)	90	16		22000	22200	1.17	0.55
PHIC-$(OH)_2$	5,100 (1.06)	150	24	PHIC-*b*-PCL_2	22200	22700	1.08	0.25
	10,900 (1.13)	90	16		21,200	22,200	1.17	0.53
	11,300 (1.19)	45	8		17000	16400	1.11	0.72
	11,300 (1.19)	90	16		22000	23000	1.12	0.53
PHIC-$(OH)_3$	5,200 (1.06)	150	24	PHIC-*b*-PCL_3	22300	23500	1.05	0.25
	9,600 (1.16)	90	16		19,900	20,600	1.09	0.50
	11,300 (1.18)	45	8		17000	16100	1.11	0.73
	11,300 (1.18)	90	16		22000	22200	1.14	0.54

[a] Polymerization conditions: monomer (M), ε-caprolactone; solvent, dry-toluene; initiator (I), PHIC macroinitiator; $[M]_0$ = 1.0 mol·L^{-1}; catalyst, DPP; $[I]_0/[DPP]_0$ = 1/1; temp., 27 ˚C; atmosphere, Ar.; conv., >99. [b] Determined by ^{1}H NMR spectrum in $CDCl_3$. [c] Determined by SEC in THF using PSt standards. [d] $M_{n,clcd}$ = ($[M]_0/[I]_0$) × conv. × (M.W. of monomer) + $M_{n,\ initiator.}$ [e] f_{PHIC} = ($M_{n,NMR,PHIC}$ / d_{PHIC})/($M_{n,NMR,PHIC}$ / d_{PHIC} + $M_{n,NMR,PCL}$/ d_{PCL}), d_{PHIC} = 1.00 and d_{PCL} = 1.15.

Electronic Supplementary Information

Precise synthesis of rod-coil type miktoarm star copolymer containing poly(*n*-hexyl isocyanate) and aliphatic polyester

Toshifumi Satoh[1,*], Naoki Nishikawa[2], Daisuke Kawato[2], Daichi Suemasa[2], Sungmin Jung[3], Young Yong Kim[3], Moonhor Ree[3,*], and Toyoji Kakuchi[1,*]

[1]Fucluty of Engineering, Hokkaido University, N13W8, Kita-ku, Sapporo 060-8628, Japan

[2]Graduate School of Chemical Sciences and Engineering, Hokkaido University, N13W8, Kita-ku, Sapporo 060-8628, Japan

[3]Department of Chemistry, Division of Advanced Materials Science, Pohang Accelerator Laboratory, Center for Electro-Photo Behaviors in Advanced Molecular Systems, Polymer Research Institute, and BK School of Molecular Science, Pohang University of Science and Technology (POSTECH), Pohang 790-784, Republic of Korea

Corresponding Authors:

*E-mail satoh@poly-bm.eng.hokudai.ac.jp (T. Satoh), ree@postech.ac.kr (M. Ree), and kakuchi@poly-bm.eng.hokudai.ac.jp (T. Kakuchi).

Table S1. Synthesis of PHIC macroinitiators (PHIC-OH, PHIC-$(OH)_2$, and PHIC-$(OH)_3$) via CuAAC reaction of PHIC-N_3 with ethynyl alcohol derivatives.[a]

PHIC-N_3		PHIC macroinitiators		
$M_{n,NMR}$[b]	M_w/M_n[c]	Structure	$M_{n,NMR}$[b]	M_w/M_n[c]
3,000	1.07	PHIC-OH	3,100	1.07
5,000	1.06		5,100	1.06
10,300	1.13		10,300	1.13
11,400	1.18		11,400	1.19
3,000	1.07	PHIC-$(OH)_2$	3,100	1.07
5,000	1.06		5,100	1.06
10,900	1.10		10,900	1.13
11,300	1.18		11,300	1.19
3,000	1.07	PHIC-$(OH)_3$	3,200	1.07
5,000	1.07		5,200	1.06
9,600	1.16		9,600	1.16
11,300	1.19		11,300	1.18

[a] Synthesis conditions: solvent, dry THF; catalyst, CuCl, PMDETA; [ethynyl derivatives]/[PHIC-N_3]/[CuCl]/[PMDETA] = 3.5/1.0/3.0/6.0 ; reaction time, 48 h; temp., r.t. [b] Determined by ^{1}H NMR spectrum in $CDCl_3$. [c] Determined by SEC in THF using PSt standards.

Table S2. Solubility of PHIC-*b*-PLLA$_{1\sim3}$, PHIC-*b*-PCL$_{1\sim3}$, and homopolymers [a]

Polymer	$M_{n,NMR}$ [b] (M_w/M_n [c])	f_{PHIC} [d]	$CHCl_3$	THF	DMF	Hexane
PLLA	10,200 (1.08)	–	○	○	○	×
PCL	10,500 (1.04)	–	○	○	○	×
PHIC	10,400 (1.11)	1.00	○	○	×	○
PHIC-*b*-PLLA	19,200 (1.07)	0.59	○	○	○	×
PHIC-*b*-PLLA$_2$	20,700 (1.12)	0.59	○	○	○	×
PHIC-*b*-PLLA$_3$	19,700 (1.08)	0.54	○	○	○	×
PHIC-*b*-PCL	20,900 (1.07)	0.53	○	○	○	×
PHIC-*b*-PCL$_2$	22,200 (1.17)	0.53	○	○	○	×
PHIC-*b*-PCL$_3$	20,600 (1.09)	0.50	○	○	○	×

[a] Conditions: temp., r.t.; concentration, 0.1 ($g\cdot L^{-1}$); ○, soluble; ×, insoluble. [b] Determined by ^1H NMR spectrum in $CDCl_3$. [c] Determined by SEC in THF using PSt standards. [d] $f_{PHIC} = (M_{n,NMR,PHIC} \times d_{PLLA\ or\ PCL})/(M_{n,NMR,PHIC} \times d_{PLLA\ or\ PCL} + M_{n,NMR,PLLA\ or\ PCL} \times d_{PHIC})$, d_{PHIC} = 1.0, d_{PLLA} = 1.20, and d_{PCL} = 1.15.

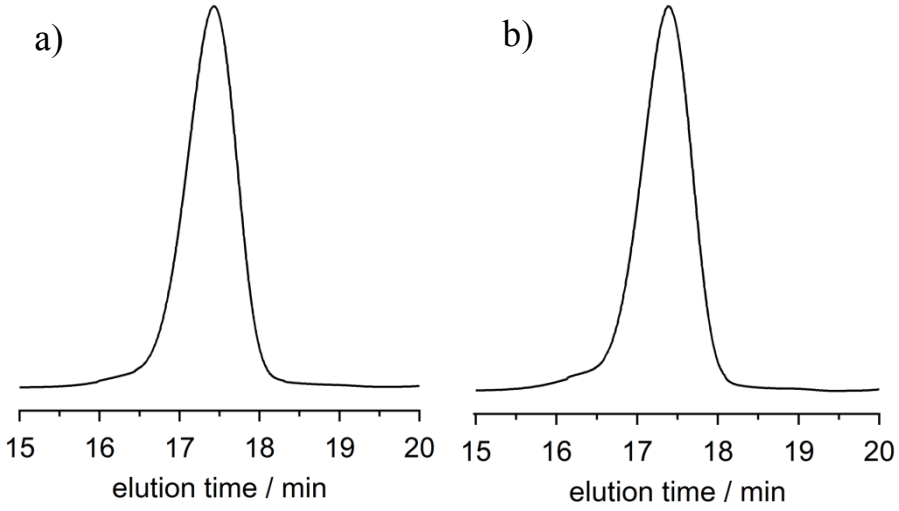

Figure S1. SEC traces of PHIC-$(OH)_2$ (a, $M_{n,NMR}$ = 5,100, $M_{w,SEC}$ = 6,100, M_w/M_n = 1.06) and PHIC-$(OH)_3$ (b, $M_{n,NMR}$ = 5,200, $M_{w,SEC}$ = 5,900, M_w/M_n = 1.06) (flow rate, 1.0 $mL \cdot min^{-1}$; solvent: THF).

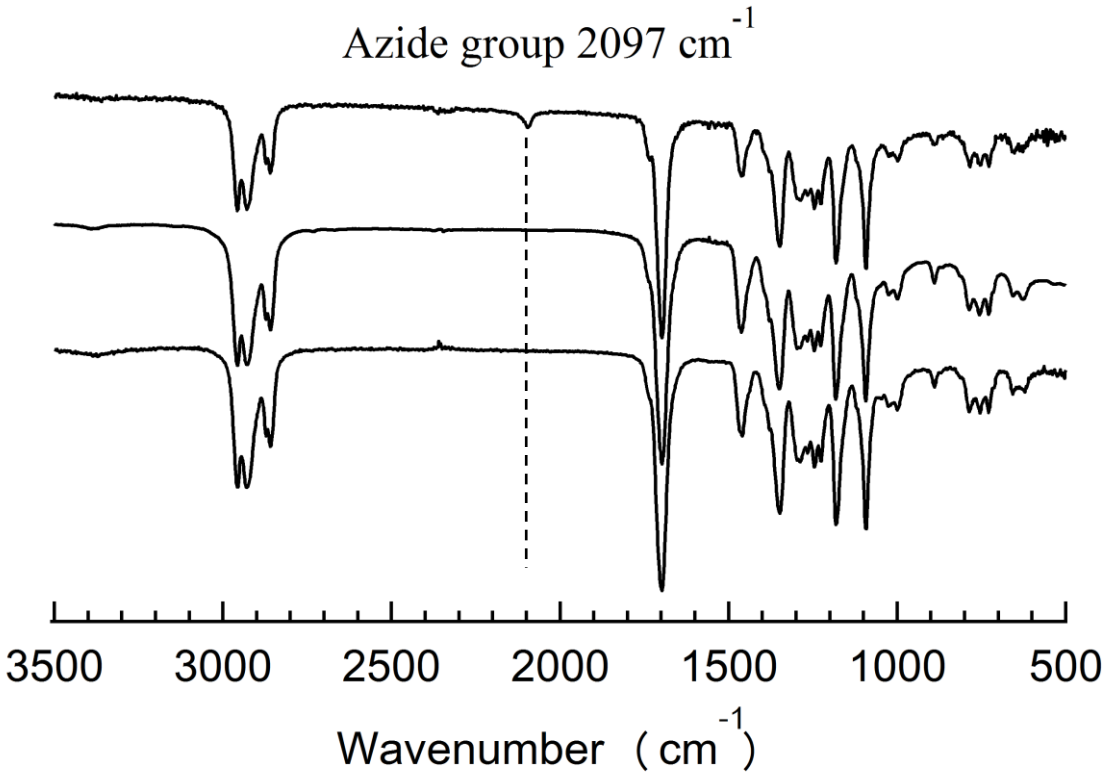

Figure S2. FT-IR spectra of PHIC-N_3 (upper), PHIC-$(OH)_2$ (middle) and PHIC-$(OH)_3$(lower).

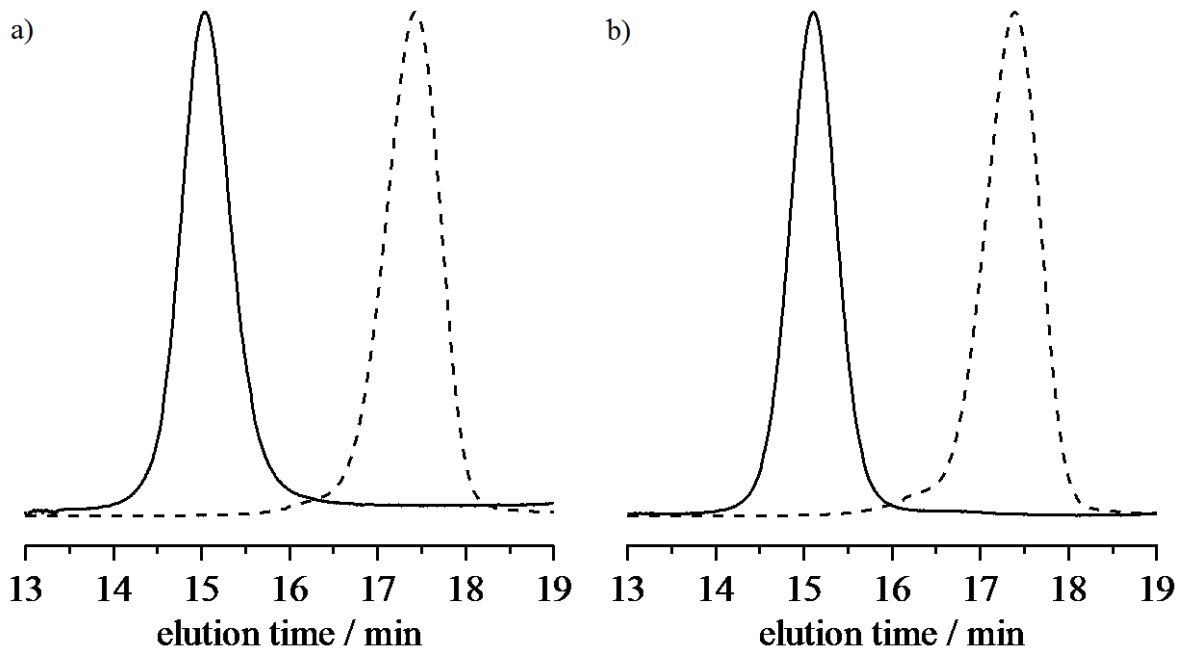

Figure S3. SEC traces detected by RI detector (eluent, THF; flow rate, 1.0 mL·min^{-1}). a) PHIC-*b*-PLLA$_2$ (solid line, $M_{n,NMR}$ = 20,000, $M_{w,SEC}$ = 23,300, M_w/M_n = 1.09) and PHIC-(OH)$_2$ (dashed line, $M_{n,NMR}$ = 5,100, M_w/M_n = 1.06), b) PHIC-*b*-PLLA$_3$ (solid line, $M_{n,NMR}$ = 20,200, $M_{w,SEC}$ = 22,800, M_w/M_n = 1.08) and PHIC-(OH)$_3$ (dashed line, $M_{n,NMR}$ = 5,200, M_w/M_n = 1.06).

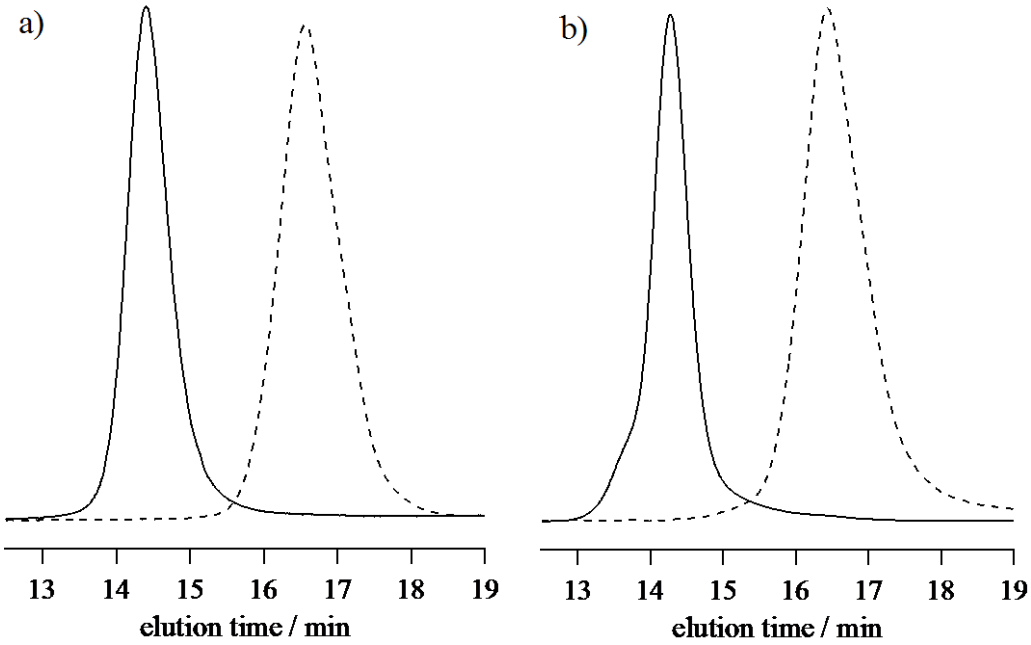

Figure S4. SEC traces detected by RI detector (eluent, THF; flow rate, 1.0 mL·min^{-1}). a) PHIC-*b*-PCL$_2$ (solid line, $M_{n,NMR}$ = 21,700, $M_{n,SEC}$ = 35,700, M_w/M_n = 1.06) and PHIC-(OH)$_2$ (dashed line, $M_{n,NMR}$ = 5,500, M_w/M_n = 1.10), b) PHIC-*b*-PCL$_3$ (solid line, $M_{n,NMR}$ = 23,600, $M_{n,SEC}$ = 37,600, M_w/M_n = 1.09) and PHIC-(OH)$_3$ (dashed line, $M_{n,NMR}$ = 5,600, M_w/M_n = 1.11).

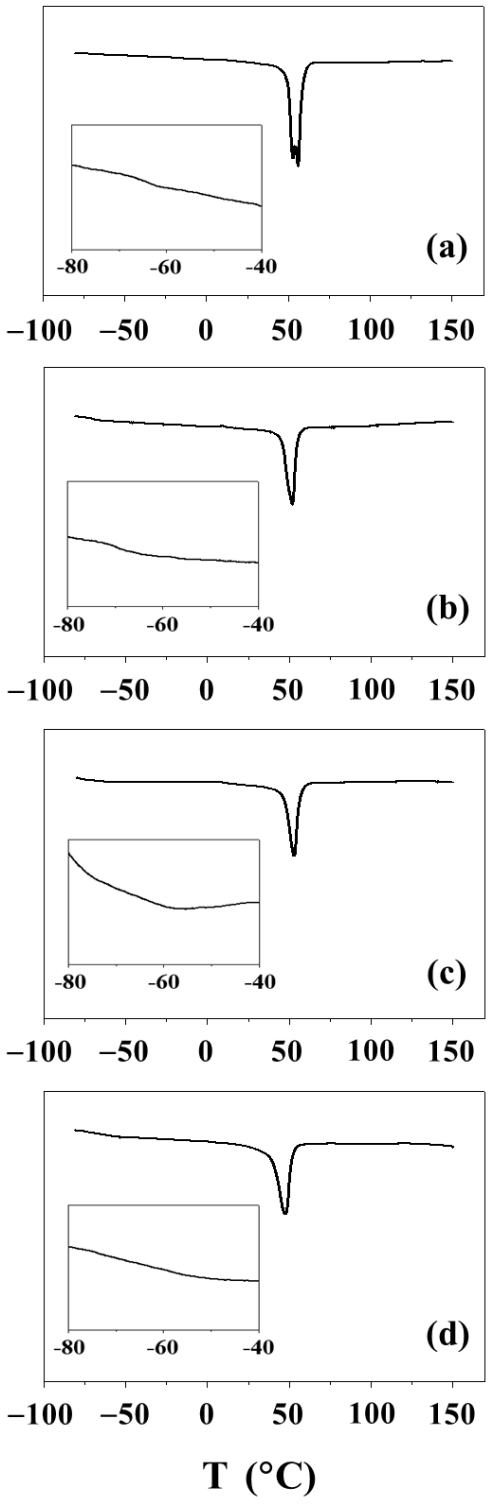

Figure S5. DSC results of PCL and PHIC-*b*-PCL$_{1\sim3}$, which were measured during heating run with a rate of 10.0 °C min^{-1} after quenched to −100 °C from the melt: (a) PCL (M_n = 10,000); (b) PHIC-*b*-PCL ($M_{n,NMR}$ = 22,200, M_w/M_n = 1.17, f_{PHIC} = 0.55); (c) PHIC-*b*-PCL$_2$ ($M_{n,NMR}$ = 23,000, M_w/M_n = 1.12, f_{PHIC} = 0.53); (d) PHIC-*b*-PCL$_3$ ($M_{n,NMR}$ = 22,200, M_w/M_n = 1.14, f_{PHIC} = 0.54).

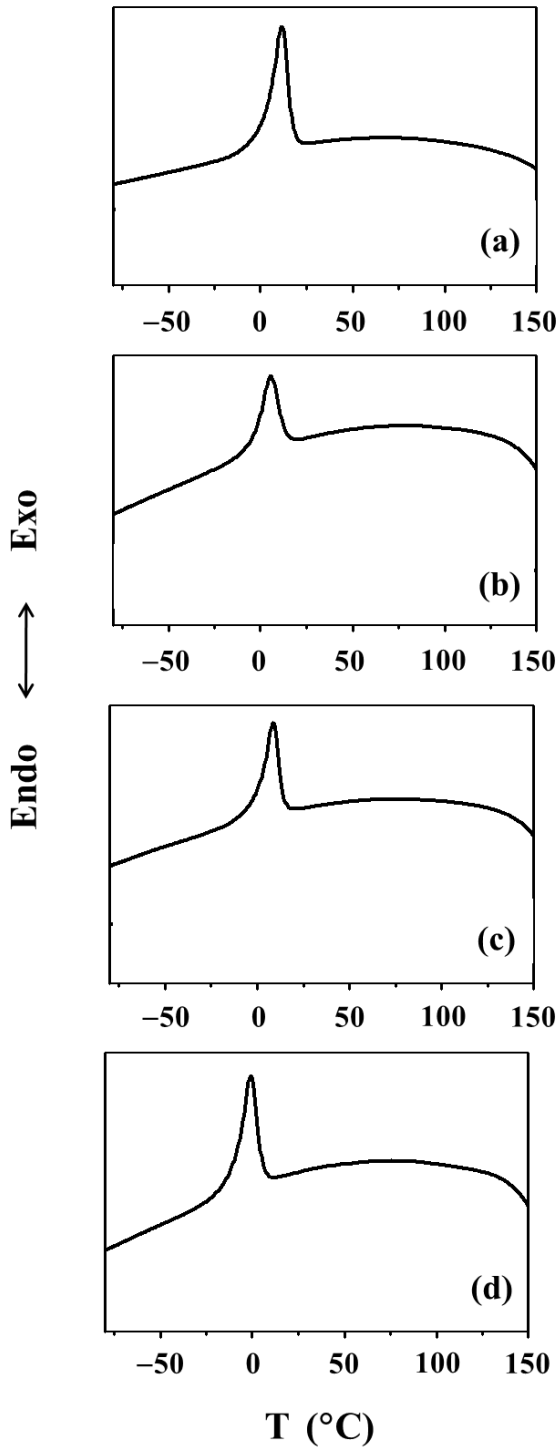

Figure S6. DSC results of PCL and PHIC-*b*-$PCL_{1\sim3}$, which were measured during quenching from from the melts: (a) PCL (M_n = 10,000); (b) PHIC-*b*-PCL ($M_{n,NMR}$ = 22,200, M_w/M_n = 1.17, f_{PHIC} = 0.55); (c) PHIC-*b*-PCL_2 ($M_{n,NMR}$ = 23,000, M_w/M_n = 1.12, f_{PHIC} = 0.53); (d) PHIC-*b*-PCL_3 ($M_{n,NMR}$ = 22,200, M_w/M_n = 1.14, f_{PHIC} = 0.54).